

Experimental Determination of the Effectiveness of Biobased Textile Reinforced Concrete

Liam Flanagan

HZ University of Applied Sciences

Final report version 1  
June-2020

## Table of Contents

Table of Contents	2
<b>Introduction</b>	<b>4</b>
1.1 Background	4
1.2 Problem Statement	6
1.3 Goals and objectives	6
1.4 Structure of this report	7
<b>Theoretical Framework</b>	<b>8</b>
2.1 Textile Reinforced Concrete characteristics	8
2.1.1 The concrete matrix	8
2.1.2 Textile reinforcement	11
2.1.3 Microstructures	12
2.2 Types of textiles	13
2.2.1 Carbon fibre	13
2.2.2 AR Glass Fibre	14
2.2.3 Bio Based textiles	16
2.2.4 Preliminary comparison between textiles	18
2.3 TRC Current applications	19
2.4 Catenary curve in construction	21
2.5 Schedule of requirements for the design of a (biobased) TRC pavilion	23
2.5.1 Functional requirements	24
2.5.2 Technical requirements	24
2.5.3 Boundaries and limitation	25
2.6 Selection of the textile for the design and construction of the pavilion	25
<b>Methodology</b>	<b>26</b>
3.1 Desk research	27
3.1.1 Literature review	27
3.1.2 Multi criteria analysis	27
3.2 Experiments	27
3.2.1 Concrete matrix tests	27
3.2.1.1 Workability	27
3.2.1.2 Air content	28
3.2.1.3 Density	29
3.2.1.4 Compressive strength test	29
3.2.2 Textile reinforced concrete tests	30

3.2.2.1 Construction of the TRC specimens	30
3.2.2.2 Uniaxial tensile test	31
3.2.2.3 Three point bending test	32
3.3.1 Shape finding	35
3.3.2 Load calculations	36
3.3.2.1 Structural self-weight	36
3.3.2.2 Snow load	37
3.3.2.3 Wind load	38
3.3.3 Buckling checks	44
3.3.4 Crack control in the arch.	48
3.3.5 Stability check	49
3.3.5 Load combinations and factors	49
<b>Results</b>	<b>51</b>
4.1 Results and discussion of MCA	51
4.2 Results and discussion of lab testing	52
4.2.1 Consistency test	52
4.2.2 Air content test	53
4.2.3 Density	53
4.2.4 Compressive test	54
4.3 Results and discussion of pavilion design	55
4.3.1 Buckling checks	57
4.3.2 Crack control	58
4.3.4 Stability check	58
<b>Discussion and Conclusions</b>	<b>59</b>
<b>Recommendations</b>	<b>60</b>
<b>Bibliography</b>	<b>61</b>
<b>Appendices</b>	<b>66</b>
Appendix 1	66
Appendix 2	68
Appendix 3	69

# 1. Introduction

## 1.1 Background

Concrete has been involved in the construction industry since before the Roman times but became utilized in a widespread manner by the Romans starting in 600BC and has become one of the most widely used materials in the world. Since then the mixture ratios, the materials used in the mixture, and the type of reinforcement used have been continually altered and improved.

Due to its compressive strength and overall image, concrete has been referred to as liquid stone in many regards as its properties match those of its solid counterpart; whilst this serves well for compressive forces applied to it, it is not the same in its tensile strength. That is the reason for the requirement of reinforcement in construction. The use of reinforcements in concrete is done for multiple factors; this includes the tensile strength of the material compensating for the lack of tensile strength of the concrete. Additionally, if the tensile strength should be exceeded, the ductility of the reinforcement will act as a form of safety as it will show the signs of this failure in the form of cracking of the concrete before reaching ultimate failure (Nawy, 2000).

The most common form of reinforcement in concrete is in the form of steel rebar that has concrete poured around it whilst the concrete is still in liquid form, the concrete is then left to set with the rebar remaining inside it. Despite the popularity of the material, there are some disadvantages connected with the use of rebar:

- The requirement of cover for steel rebar can be expensive and time-consuming to the project as well as adding additional size to the cast concrete (Cauberg et al., 2012).
- There is a limit to the shapes that are possible to produce as it is very expensive and labour intensive to shape rebar, especially alternative shapes to the standard block shape (Cauberg et al., 2012).
- The costs of rebar when compared to alternative methods, such as textile reinforcement, are a lot higher (Cherkas et al., 2017)
- Steel reinforcement is susceptible to external stimuli such as heat, electric, magnetic and environmental corrosion e.g. oxidation. (Cherkas et al., 2017)

Since the end of the 20th century research groups around the world from Germany (Curbach et al., 1999, Bramshuber, 2006, Scheerer et al., 2015), United Kingdom (Ohno et al., 1994) and Japan (Hayashi et al., 1990, Fujisaki et al., 1993) have been looking into continuous and woven fibres being used in cementitious materials. It has since spread to the rest of the world and now textile reinforcement has provided an alternative to the use of steel reinforcement. Textile reinforced concrete (TRC) can be defined as a composite material consisting of mixtures of cement, mortar or concrete, and discontinuous, discrete, uniformly dispersed suitable (synthetic or natural) textiles. The use of TRC allows many advantages:

- Taking up less space when used in concrete so less need of cover/you can achieve very thin layers or structures (Cherkas et al., 2017).
- Malleable nature (Cauberg, et al. 2012).
- Possibility to design spatial structures (De Bolster et al., 2009).
- No risk of corrosion, since no textile is steel-based (Williams Portal, 2015).

Whilst synthetic textile such as carbon fiber and AR-glass textiles are broadly analyzed in literature, little is known about the use of natural textiles in TRC.

This thesis looks at the use of natural textiles in TRC and it is part of the HBO-postdoc research by Dr G. Scuderi, PhD. This postdoc is looking into the use of biobased materials in combination with concrete, to create new materials or technologies able to improve the current construction climate. This is in conjunction with another thesis on biobased concrete written by Rami Toubassi. The HBO-postdoc is undertaken at the Biobased Building research group (Biobased Bouwen Lectoraat), part of the Centre of Expertise Biobased Economy. The research group collects, develops, valorizes and disseminates knowledge about the application of biobased materials in construction and civil engineering.

In this research three different natural textiles are expanded upon, namely ampliTex™, powerRibs and Jute. The first being a flax-based material woven in a bi-directional fashion at 0° and 90° to achieve a fabric with a low environmental impact and a high laminate stiffness. The second being a flax-based material that is a composite due to it being reinforced with plastics. The third being a Jute textile with a density of 275g/m<sup>2</sup>. These materials have been found to have lower water usage, CO<sub>2</sub> footprint, and embodied energy than that of the commonly used carbon fibre reinforcement (Mathijssen, 2018).

This research focuses on the application of the textiles mentioned above in TRC technologies, through desk research and the design of specific lab testing techniques, to establish their effectiveness in the construction field. This being done in terms of strength, cost and ease of application.

Originally, the thesis period entailed carrying out strength and durability tests upon the aforementioned biobased TRC. However, due to the Covid-19 outbreak in the Netherlands and the consequent closure of the laboratory, the scope of the research has been reconsidered.

The present thesis focuses on the desk research and design of the laboratory tests for biobased TRC, however carrying out the tests and analysing the results is out of the scope of the current work. A design of a pavilion that makes use of this technology is also looked at, attempting to find a way to construct it in a way that plays to the strengths of the materials involved. The pavilion is designed as a catenary curve, as it is a way of designing a structure that is purely in compression when it is under its self-weight, which compliments the use of textile reinforcement in construction as well as allowing for an aesthetic look (Block et al., 2006). In this thesis, the textile reinforcement of the pavilion is realized with carbon fibers. This choice has been made due to the availability of literature data. Again, the purpose of this design is to find a suitable application for TRC, which could be suitable also for the use of biobased textiles.

## 1.2 Problem Statement

The construction industry has a large environmental impact and this needs to be reduced and negated as much as possible in order to ensure the sustainability of life on Earth (Sharrard et al., 2008). Many different methods are being deployed attempting to reduce the impact the construction industry has on the environment. This research focuses on using sustainable materials and on UN Sustainable development goals number 12 (Responsible construction and production) and number 13 (Climate action).

As mentioned previously concrete is one of the most widely used construction materials in the world, producing most of the CO<sub>2</sub> emissions and using the most resources, such as sand (Benhelal et al., 2013). In the structural design of concrete constructions, rebar and reinforcement have a strong impact, as they are necessary to the tensile strength of the construction. This is usually steel reinforcement as it is universally seen as the reinforcement solution (ACI Education Bulletin E2-00, 2000). This rebar also requires a certain amount of coverage to ensure that it does not oxidize or erode due to contact with outer stimuli, such as water, oxygen and corrosive liquids such as acids (EN 1992-1-1, 2008), this adds excess concrete volume requirements to the project .

The use of concrete can be reduced with the use of textile reinforcement, as it does not possess the same restrictions as steel in terms of cover (Cherkas et al., 2017). Additionally, the environmental impact of the material can also be reduced by using a textile that is biobased and more environmentally friendly. The problem is that despite the tensile strengths of biobased textiles being known, the effectiveness of biobased textile-reinforced concrete is still unknown. This is due to the nature of biobased textiles, and due to the uncertainties about the compatibility between the materials.

In order to determine the applicability of these bio-based textiles in TRC, specific laboratory testing must be undertaken. However, most of the time, there are no standard laboratory techniques applicable for biobased textiles and biobased TRC.

## 1.3 Goals and objectives

The goal of this research is setting up suitable laboratory tests and analysis methods for the strength and durability testing of bio-based textile reinforced concrete. With Textile Reinforced Concrete being a composite material with a heterogeneous structure, it is important to evaluate the properties of the individual materials and their composite action to gain an understanding of the composite behaviour of a structure made from it. This thesis presents also a possible application for this new technology, by developing the design of a pavilion based on the catenary curve. In this phase, the pavilion is verified by imagining a carbon fiber reinforcement. Therefore, this thesis is a preparatory research for the actual development of bio-based TRC applications.

Therefore, a main research question is developed:

- How to design a pavilion making the best use of the TRC properties and making it suitable to bio-based TRC applications?

This main question will be answered by using the following sub-questions.

- What are the benefits, limitations and costs of using biobased textile reinforcement in a construction compared with other textiles?
- How can natural textiles be used for the production of biobased textile reinforced concrete?
- What are the requirements for the design and construction of a pavilion realized with biobased textile reinforced concrete?

## 1.4 Structure of this report

In this report the following steps were taken to ensure that the research questions were answered correctly. Firstly textile reinforced concrete was researched to determine how textiles can be used to reinforce concrete and the more commonly used textiles that are used. The biobased textiles were then researched to determine whether they would be suitable for the intended uses required in this project in comparison to the more commonly used materials. After this the type of shape that would be used for the pavilion was decided upon and researched in terms of its application in construction.

Within this research there were limitations as to the process, testing and research, these were all then established in the schedule of requirements and boundary conditions.

It was then necessary to start analysing the data found in the research and comparing the data to determine the best solution to the research questions, and thus an MCA was used to evaluate each of the textiles researched in this thesis. Next came the methodology and explanations of how each aspect of the research was performed such as the literature reviews, MCA, experiments, design of the pavilion as well as the loads calculations. Once the loads were calculated it was necessary to apply these to the safety checks to determine whether the design was safe or not. Lastly the results of all the different researches expressed in the methodology were discussed to formulate a final answer to the research question.

## 2. Theoretical Framework

### 2.1 Textile Reinforced Concrete characteristics

Concrete is considered a composite material, meaning it comprises different materials, such as aggregates or particles, embedded in a medium used to bind them together. The most commonly used medium is hydraulic cement, which activates by mixing with water (Mehta, et al. 2006). This mixture is then usually used to encase the reinforcement of the structure, most commonly steel rebar. This restricts the feasibility of architectural structures due to difficulty and labour intensity to shape rebar, especially when looking for alternative shapes to the standard block shape (Caugberg, et al. 2012). With concrete being known as liquid stone, it is counterintuitive to restrict its use in such a manner. That is where the use of textile reinforcement has been shown to have promise, in that it allows for the designs of distinct and possibly more eco-friendly structures (Williams Portal, 2015). This type of composite material is commonly referred to as Textile Reinforced Concrete, further referred to with the acronym TRC. TRC is a fine-grained cement mixture encasing textile reinforcement that is woven into the form of a grid or mesh structure made of non-corrosive fibres.

TRC is different from other forms of cement-based composites, e.g. fibre reinforced concrete, or FRC, because it is made of fibres bundled and arranged in a discrete open pattern such as a grid. This grid presents a tensile behaviour similar to conventional reinforced concrete (RC) thus increasing the tensile capacity and effectiveness of the fibres in comparison to FRC, which comprises short fibres randomly distributed in concrete. Accordingly, TRC is often claimed to combine the benefits of both RC and FRC (Hegger et al., 2006). On the other hand, continuous meshes, woven fabrics and long wires or rods are not considered to be discrete textiles (Papanicolaou, & Papantoniou, 2010).

To better understand this composite material, it is necessary to study the different components of TRC. These are namely the concrete matrix as well as the textile reinforcement.

#### 2.1.1 The concrete matrix

The concrete matrix applied in TRC differs from that usually employed in standard steel-reinforced concrete. Fine-grained concrete described and or defined as mortar is often used for TRC, this is determined when the grain size is found to be less than 2mm. Self-compacting and extremely flowable concrete is primarily required to adequately pass through the holes of the textile reinforcement structure to permit adequate bonding and transfer of forces from the concrete to the reinforcement (Mehta et al., 2006). This small grain size might, however, increase shrinkage and therefore it would require bigger amounts of cement paste.

In this research a concrete mixture of cement, fly ash, silica fume, siliceous sand, ankerfill, water and a plasticizer will be used. Following, the components will be described:

- Cement (see Figure 1) being defined as an adhesive substance capable of uniting pieces or masses of solid objects/matter into a compacted whole. This is a broad definition of the term but encompasses the type of adhesive mixture used in the creation of concrete. A more accurate name for the cement used in the construction of concrete would be 'Calcareous Cement', which applies to cements that contain lime as one of its principal constituents (Hewlett, & Liska, 2019).



Figure 1: Cement

- Fly ash (see Figure 2) is a term used for a by-product produced in furnaces burning solid fuels, and with the reliance of the world on energy that is primarily produced through the burning of coal, it should be recognised that with this large production of fly ash it is necessary to dispose of it as safely and environmentally friendly as possible. Another way to look at this by-product would be as a resource to be used. The similarity of this by-product to that of volcanic ash has led to the encouragement of the use of it in concrete mixtures. There are two main types of fly ash, those being high-calcium and low-calcium. With high calcium a larger amount of lime can be found which as previously discussed is a principal constituent of calcareous cement. Therefore high-calcium fly ash when used in the capacity of concrete acts as an additional cementitious material in the mixture. (Wesche, 1991)



Figure 2: Fly Ash

- Silica fume (see Figure 3) is a non-crystalline form of silicon dioxide. This is an ultrafine powder that is a by-product of silicon and ferrosilicon alloy production. It has been tested and used as an addition to cement since 1952. It is a pozzolanic material which means that it is a material that when in a fine state and in the presence of water will react chemically with calcium hydroxide at normal temperatures to form a compound with cementitious properties. This applies to fly ash as well as siliceous sand making the concrete mixture more similar to a cementitious mortar (Mazloom, et.al, 2004).



Figure 3: Silica Fume

- The use of siliceous sand (see Figure 4) is two-fold as it works both as an aggregate and pozzolanic material in the concrete mixture. Siliceous sand is mostly constituted of silica ( $\text{SiO}_2$ ). This substance is one of the most commonly found elements in the world and is mostly commonly found in quartz form. Its quartz composition is known for its very strong resistance to chemical and physical attack (Ineson, 1990).



Figure 4: Siliceous Sand

- The use of ankerfill (see Figure 5) was used in this research as a substitute for basalt flour which is used in a similar manner to fly ash and silica fume as a means of replacing some of the cement that would normally be required as a way of reducing the carbon footprint of the concrete and is known for distributing loads well (Kutschera et al., 2009).



Figure 5: Ankerfill

In this research a ratio was decided on to remain consistent throughout the tests. This ratio can be found below.

Cement CEM I 52.5 R(c)	22.2%
Fly ash	7.9%
Silica fume	1.6%

Water	12.7%
Superplasticizer	0.5%
Anker fill	22.7%
Siliceous sand	32.4%

Table 1: Mixture ratios

### 2.1.2 Textile reinforcement

Textile reinforcement is defined as a composite material composed of a heterogeneous structure. To understand the complicated behaviour of this material, it ought to be examined at several empiric levels, e.g. macroscopic to microscopic. Fibres are categorised in line with their origin as being either biobased, e.g. jute and flax, or synthetic, e.g. nylon, carbon and glass (Fangueiro, 2011). The assembly differs based on the character of the fibre, i.e. inorganic or organic. Fibres may be used to produce individual fibres of continuous length, likewise referred to as filaments, which are characterized by a diameter of between 7-27  $\mu\text{m}$  conditional on the textile kind (Bentur et al., 2006, Brameshuber, 2006). A filler material is usually applied to the filaments to ensure surface protection and improve the interaction between them in an assembled cluster (Dejke, 2001). The grouping of continuous filaments may be achieved by either twisting or grouping filaments along in a parallel manner. Based on the application, the description differs, whereby yarn usually describes the cluster of twisted filaments, whereas tow or roving denotes bundled filaments in parallel. The parallel filament bundles are usually used for reinforcing applications as they give smaller structural elongation as compared to alternative sorts of assemblies (Brameshuber, 2006). For improved bond in concrete, the surface options and volume of a yarn may be changed by texturing or crimping (the addition of supplementary crimps, coils or loops along its length) (Fangueiro, 2011). What is more, the quantity of filaments incorporated in a bundle relies on the required finish thickness (Mahadevan, 2009), strength properties and application. The fineness of a yarn is measured in tex ( $\text{g}/\text{m}^2$ ) and is a result of the quantity of filaments, average filament diameter and density. Fibres may be additionally bundled to form textile structures using varied strategies to supply nonwoven, woven, braided or meshed materials. Regardless of the grouping technique, textile reinforcement is usually classified as being two-dimensional (planar) or standard (2D) (see Figure 6), three-dimensional (3D) (see Figure 7), directionally orienting (DOS) or hybrid structures.

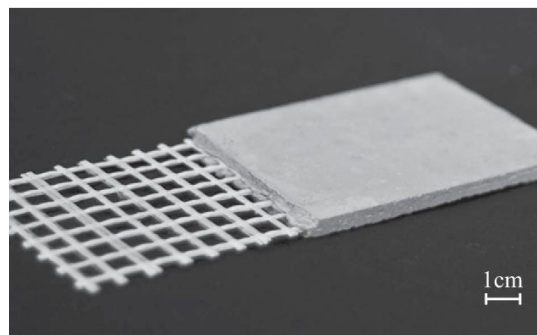


Figure 6: Example of 2D textile reinforced concrete

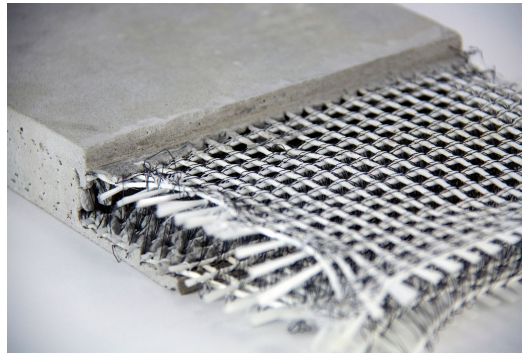


Figure 7: Example of 3D textile reinforced concrete

These structures are additionally described according to the direction of the yarns/rovings: mono, bi-, tri- or multi-axial (Fangueiro, 2011). Within the case of a bi-axial case, the mesh/grid includes 2 types of yarns/rovings, warp ( $0^\circ$ ) and yarn (or fill) ( $90^\circ$ ), interconnected orthogonally. This is the type of fibre reinforcement that will be explored in this project.

### 2.1.3 Microstructures

TRC is differentiated from normal steel reinforced concrete chiefly due to its advanced heterogeneous structure (Möller et al., 2005; Häußler-Combe et al., 2007). A textile reinforcement yarn consists of multiple fibres that inhibit the penetration of the fine-grained concrete matrix in between the filaments. The inner filaments, as a result, have less contact with the fine-grained concrete matrix reliant on the scale of the gaps between fibres. The ‘fill-in zone’ is the depth at which the adhesive load transfer will take place between the filaments and above mentioned matrix. The inner zone, i.e. core, is outlined as the filaments having less contact with the matrix however assuming that resistance load transfer between the filaments remains attainable (Hartig et al., 2008). The yarn structure embedded in a concrete matrix as well as these above-mentioned associated zones is conceptualized in Figure 8.

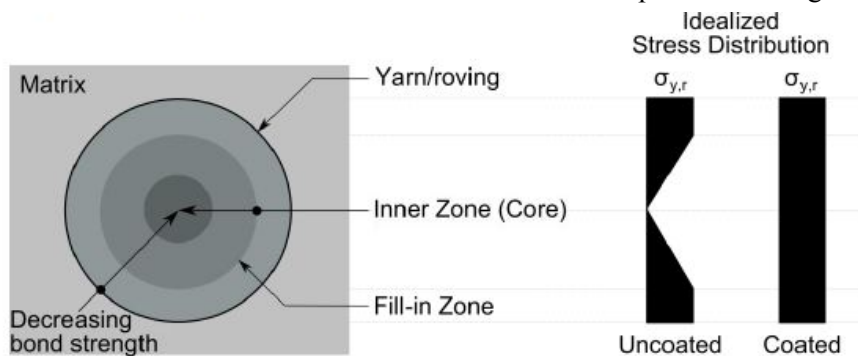


Figure 8: Conceptualized yarn structure

The heterogeneous bond between the textile reinforcement mesh/grid and matrix will differ greatly depending on, e.g. fibre type, binding sort, surface smoothness, and rheology of the concrete matrix. The

impregnation of the textile mesh/grid applying, e.g. polymer-based coatings, is usually employed to eliminate the extremely heterogeneous structure of the yarn/roving. The penetration of the coating into the yarn/roving activates a lot of internal filaments, this successively improves the load transfer between the filaments (Morales Cruz et al., 2015). Ideally, the aim is to activate the whole yarn/roving to achieve a continual stress distribution across the yarn/roving cross-section as illustrated in Figure ... (above). This configuration may be seen as analogous to a homogenous bond surface between the cement matrix and reinforcement. Increased bond strength and composite tensile strength because of additional surface coatings has been described in varied studies, e.g. in Büttner et al. (2008) and Scheffler et al. (2009c). The modification of the surface roughness utilising sand fillers and coatings has additionally been found to positively impact the bond (Morales Cruz et al., 2015). Coatings applied to entire sections of textile reinforcement mesh/grid will therefore influence the stiffness and draping characteristics. Alternative improvements comprise additional surface protection throughout handling and in the alkaline environments.

## 2.2 Types of textiles

### 2.2.1 Carbon fibre

Carbon fibres (see Figure 9) are artificial chemical fibres which will be made using 2 methods: 1) meso phases pitch (petroleum) and 2) based on polyacrylonitrile (PAN). Production technique two is mentioned here as this is most ordinarily employed in TRC applications; but, every technique aims for carbon fibres having a minimum of ninety percent carbon content (Wulfhorst et al., 2006). The production of carbon yarns involve the subsequent processes (Brameshuber, 2006, Wulfhorst et al., 2006):

- > Wet-spinning, i.e. polymerisation, of organic compound organic compound polyacrylonitrile → chemical fibres
- > Thermal stabilization of fibres (200-300 °C), i.e. removal of non-carbon atoms through chemical reaction → unmeltable fibres
- > destructive distillation and graphitization of fibres (1000-3000 °C), i.e. aligning graphite layers parallel to fibres → carbon fibres from PAN, i.e. High perseverance (HT)-fibres (1500-1700 °C) or High modulus of snap (HM)-fibres (2200-3000 °C)
- > Drawing of processed fibres → filament (Ø seven to fifteen µm)
- > Sizing/coating on filaments
- > Bundling of filaments → yarns/rovings

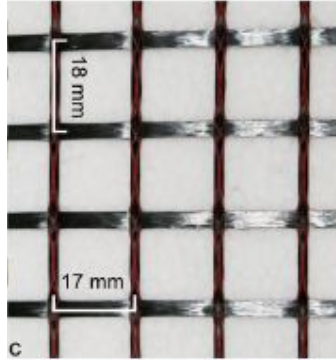


Figure 9: Carbon fibre textiles

Carbon fibres are often made up of totally different parts, i.e. PAN and pitch, as mentioned above, wherein the configuration controls the characteristics of the fibres (Dejke, 2001). Most styles of carbon fibres, e.g. PAN and high performance pitch have been shown to be resistant to acids, bases and organic solvents (Machida et al., 1993). Likewise, carbon fibres have been usually classified as being inert with chemicals (Micelli et al., 2004, Scheffler et al., 2009), to the extent that they will be applicable in environmental exposure. For instance, when immersed in a basic solution (NaOH) for twenty eight days, carbon fibres were marked by tensile strength as well as loss of volume and an absence of reaction materials on the surface (Sim et al., 2005). Remarkably, a small increase of strength when undergoing accelerated testing was discovered for carbon fibres by e.g. Hegger et al. (2010). Relating back to carbon-FRC, Katz et al. (1996) discovered that HM-PAN carbon fibres embedded in a concrete mixture went up in strength and toughness throughout the early ages (< thirty days) that was followed by a loss in mechanical properties as a result of matrix densification.

The tensile strength of carbon fibre varies widely based on the manufacturing of the fibre. These can vary in multiple aspects such as high tensile strength (3–7 GPa), high tensile modulus (200–935 GPa), compressive strength (1–3 GPa), and compressive modulus (100–300 GPa), as well as low density (1.75–2.20 g/cm<sup>3</sup>) (Newcomb, & Chae, 2018).

Carbon fibre is also widely known as being one of the most costly forms of reinforcement in the construction industry (Gill et al., 2016). It can cost up to \$15/kg in comparison to stainless steel or aluminium which typically cost around \$1.5/kg. This is a very large gap and it is one of the main reasons for the limited use of the material despite its high tensile strength and workability.

### 2.2.2 AR Glass Fibre

AR-glass is commonly known as the most price effective and most easily accessible textile Reinforcement, especially if compared to carbon fibres (Büttner et al., 2010). Glass fibres are derived from inorganic non-metallic raw materials to produce chemical fibres (Wulfhorst et al., 2006). The raw materials required to make AR-glass are primarily silicon dioxide sand (SiO<sub>2</sub>) and up to 15-16 wt-% zirconia (ZrO<sub>2</sub>) to produce a superior alkali resistance (Bentur et al., 2006; Brameshuber, 2006). These quantities are then proportioned through a batching method.

The manufacturing of AR-glass yarns carries with it the subsequent processes (Brameshuber, 2006; Wulfhorst et al., 2006):

- > Melting method of raw materials between 1250-1350 °C → melted glass
- > Fiberization of melted glass, i.e. wet-spinning method (25-150 m/s) → filaments (Ø 9-27 µm)
- > Sizing/coating (organic polymers) on filament → surface wetting and bonding of filaments (Parnas et al., 2007).
- > Bundling of filaments → yarns (e.g. 400-6600 range of filaments)

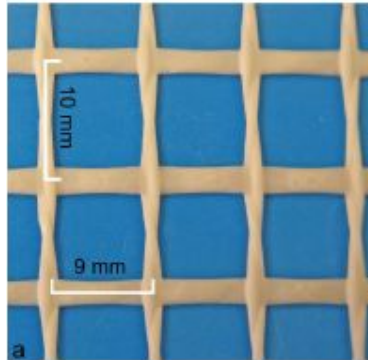


Figure 10: AR glass fibre textiles

AR-glass fibres (see Figure 10) bear strength loss when encased in cementitious mixtures over a lengthy period of time (Purnell, 1998). These fibres are actually facing a similar deterioration mechanisms experienced by glass-fibre concrete (Butler et al., 2009). Hydroxide ions (OH<sup>-</sup>), found in a base solution, react with the silica compounds (Si-O-Si) of the glass fiber network that build up wet surfaces. The ions finally break down silica (Scheffler et al., 2009c). What is more, thanks to the assembly method, the AR-glass fibre surface is marked by tiny defects and/or weak zones that cause strength loss. Consequently, these supposed weak areas allow for local displacements, pitting corrosion and stress concentrations once placed in a basic or alkaline atmosphere (Purnell, 1998, Orłowsky et al., 2005). As mentioned above the cost of glass fibres is lower than that of carbon fibre. The price of AR glass fibre averages at about \$3.43/kg (Shakor, & Pimplikar, 2011). This is less than a quarter of the price of carbon fibre.

Due to glass being recyclable it is possible to use recycled glass as up to 40 % of the glass fibre (Majumdar, et al., 1977). This impacts the effect that the production of the fibres has on the environment and the overall CO<sub>2</sub> footprint.

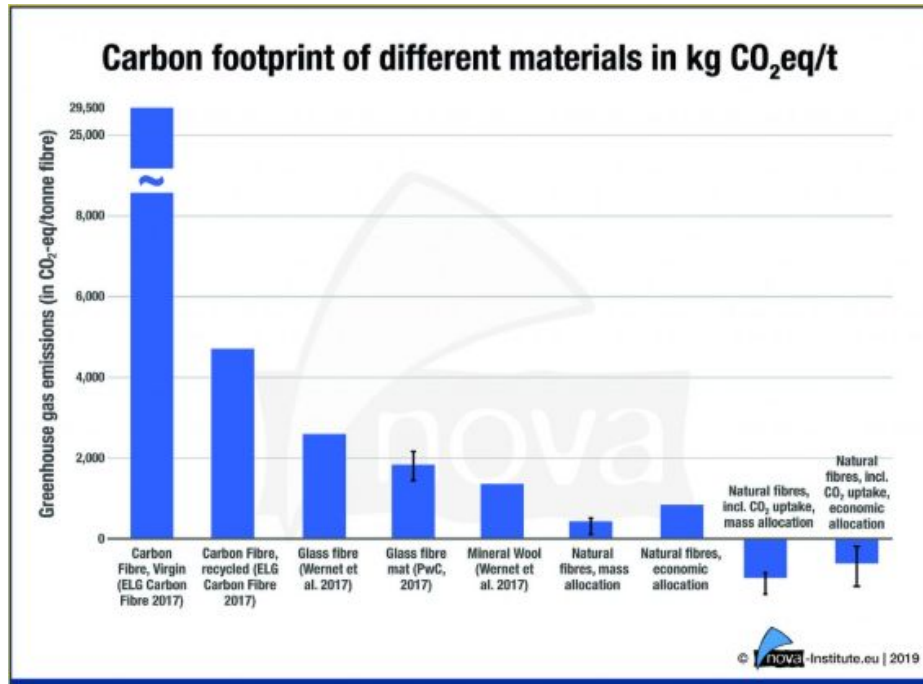


Figure 11: Carbon footprints of different materials

### 2.2.3 Bio Based textiles

Natural textile industries provide millions of jobs around the world, especially in the developing countries. Natural textiles are the major non-food natural artefact, and they are processed in several little and huge industries and shoppers around the world. The promotion of the use of natural textiles as a CO<sub>2</sub> neutral resource is believed to contribute to a greener planet (van Dam, 2008).

In the reinforced concrete industry, changing to a bio-based reinforcement means substituting common raw materials currently largely produced from mining of metal or mineral resources, with products produced from renewable (plant and animal based) resources.

Natural textiles are defined as bio-based fibres or fibres from vegetable and animal origin woven into textile form. This definition includes all natural plastic fibres (cotton, jute, sisal, coir, flax, hemp, abaca, ramie, etc.) and primarily protein based fibres like wool and silk.

In this research, three natural textiles are analysed, namely ampliTex™, powerRibs and Jute, each with its own characteristics.

To analyze their suitability for biobased TRC, it is important to compare them with each other individually, outside of the concrete mixture, as well as with the more commonly used materials in use in TRC at present.

AmpliTex™ (see Figure 12) is a fabric or textile made of flax fibres with high tensile strengths as well as elastic modulus, which makes them performing technical fibres. These types of natural fibres fall under the bast category. AmpliTex™ is known as a good vibration dampener as well as having a low fragile fracture behaviour when compared to carbon fibre. This material also has a near zero coefficient of

thermal expansion. Being made of flax means that this product has a negative global warming indicator due to its CO<sub>2</sub> sequestration by photosynthesis. This is found to be true in the powerRibs as well.



Figure 12: AmpliTex

PowerRibs (see Figure 13) are a textile material made of flax fibres as well, and designed to be used as a part of a composite. When it is part of a composite it increases the flexural stiffness and damping properties of the composite with minimal additional weight added to it. The design of the material itself is inspired by the veins found in leaves and how they hold the structural self weight of the leaf. Due to the powerRibs grid structure and the size of the yarns it has a high damage tolerance and also ensures that if the composite breaks all pieces will be held together.

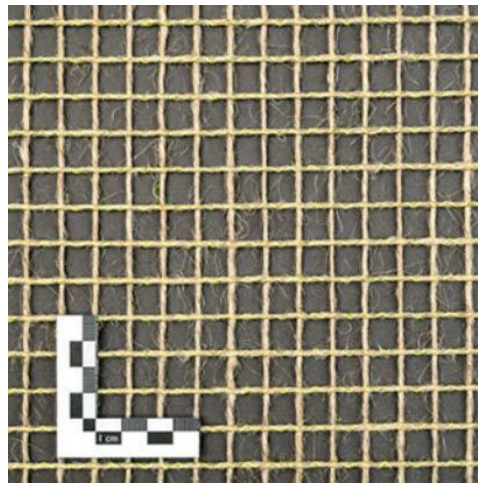


Figure 13: PowerRibs

Jute (see Figure 14) is a natural fibre commonly used and widely produced, second only to cotton in terms of production quantity. This fibre has been a staple in textile production since the 3rd millennium BC. It is a natural fibre that falls into the bast category with flax as well, and has very low requirements in terms of water and pesticides in comparison with its main textile competitor, cotton. Jute is also known for being very inexpensive and having a high tensile strength for natural fibres (Sett et al. 2000).



Figure 14: Commonly used jute textiles

Natural fibres contain multiple saccharides, which may affect the hydration of cement in a negative manner. However, they do not all have the same repressive result. The amount and concentration of saccharides in every fibre depends upon not solely the sort of natural fibre, but also the environment within which they were grown. According to the research the negative effects are mainly contributed by the absorption of the clinker grains by the fibre (Kochova et al. 2016; Na et al. 2014). Saccharides have multiple properties, but the main properties that affect the compatibility are the alkaline stability of the fibres and their ability to bind with calcium. Research has shown that the saccharides are subject to hydrolysis when they are subject to an alkali environment like that of cement paste (Thomas & Birchall 1983). The effect of this hydrolysis is the retarding of the concrete's setting time drastically. This can be counteracted with the use of pretreatments and coatings.

#### 2.2.4 Preliminary comparison between textiles

As can be seen in table 2, the carbon fibre and glass fibres out perform the biobased textiles in tensile strength and tensile modulus. The density of the materials however negatively impact their effectiveness as they will have a larger self-weight than the biobased textiles when being used in the same capacity.

Textile	Density(kg/m <sup>3</sup> )	Tensile strength(MPa)	Tensile modulus(GPa)
ampliTex	1450	149.3	19.4
powerRibs	363.6	280	3.45
Jute	275	345	2.7
Carbon Fibre	1770	3950	238
AR Glass fibres	2550	1956	78.51

Table 2: Different textile reinforcement types and their attributes. (Asokan et al. 2012, Fu et al. 2000)

If Carbon and AR glass fibres are better in terms of strength, in terms of environmental effects the flax fibres outperform them to a large degree (Figures 15, 16 and 17). This reduction of environmental impact is what is necessary to better the construction industry as a whole to make it more sustainable.

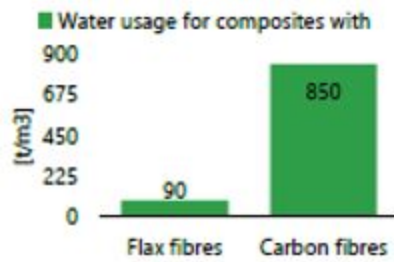


Figure 15: Water Usage

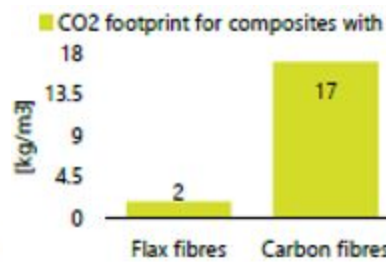


Figure 16: CO2 footprint

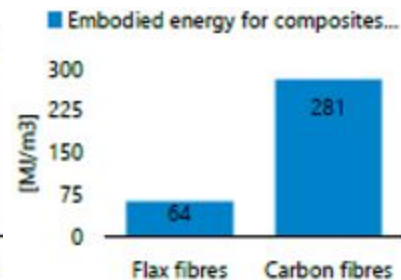


Figure 17: Embodied Energy

According to Figures 18 and 19 the values of CO2 Footprint and Embodied energy for the glass fibres are larger than for ampliTex flax. This shows that the glass fibres have a larger impact on the environment.

Greenhouse gas emissions

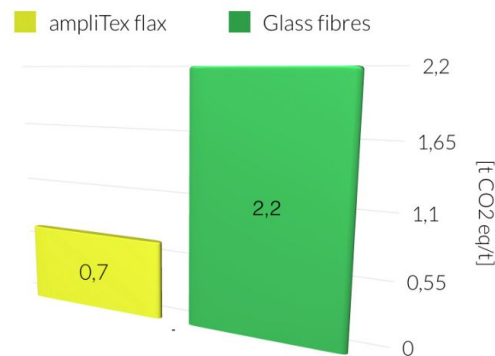


Figure 18: CO2 Footprint

Non-renewable energy consumption

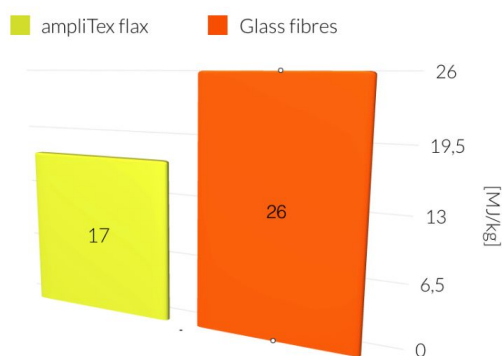


Figure 19: Embodied energy

The pricing of natural textiles is another factor that works in their favor as they are known for being relatively cheap when compared to the synthetic textiles. These prices range from \$0.54-0.65/kg, which means that they are six times cheaper than AR glass fibres and 30 times cheaper than carbon fibres (Karus, & Kaup, 2002).

## 2.3 TRC Current applications

Currently the main applications of textile reinforced concrete are in the field of facades, self supporting sandwich elements and shell structures.

In terms of the facades themselves TRC permits economic savings in terms of elements, transport and anchorage prices and so has been used for thin-walled and lightweight aired façade systems in recent years (Hegger et al. 2006; Brameshuber 2006). At present, tiny panel sizes of 0.5–3 M<sup>2</sup> are being used in application of TRC in Germany for example. Panel sizes of up to seven M<sup>2</sup> will solely be complete together with bracing stud-frame systems (Engberts 2006). Due to the missing style codes the appliance of TRC façade components needs either specific approval for every construction or a general approval for outlined boundary conditions.

With self supporting sandwich elements the force bearing capacity is primarily dependent on the thickness and overall height of the panel as well as the stiffness of the core. These are commonly applied in factory or industrial settings in order to reduce the overall thickness of outer layer panels by 5-6 cm as it requires less cover than standard reinforced concrete (Hegger et al. 2008). When these are used inside facing they are constructed in conjunction with rigid heat resistant polymers as a form of insulation.

The shell structures that are constructed will be looked at closely as it fits into the design to be used for the pavilion. Due to its material properties TRC is useful in the assembly of advanced geometries, e.g. for roof constructions. The bearing capacity will be improved particularly by the formation (bending or folding) of two-dimensional building components. The simple forming of the textiles allows an easy realization of circular surfaces. Even in reinforced concrete structures, simple channel-section crimped beams belong to the foremost economical kinds of construction. The shell result of skinny concrete components is effective within the case of barrel-shell roofs. With a fabric thickness of 25mm in textile-reinforced concrete the structure is extraordinarily light-weight as well as the shell being rigid in both the longitudinal and lateral direction. It is possible to generate fascinating forms of applications for this sort of TRC structure with a span of up to 8m , e.g. in smaller and medium-sized halls. The employment of shotcrete is the best production technique for TRC shells with the location of concrete and reinforcement in alternating layers. The production of such a barrel shell was with success tested on a one.5 m long phase at the Institute of Buildings Materials analysis (ibac), RWTH Aachen University (Chudoba et al., 2016).

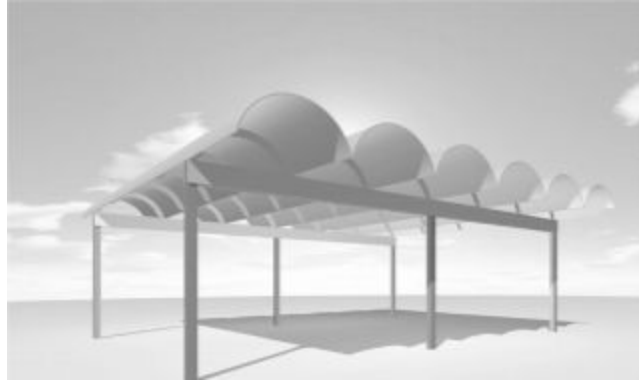


Figure 20: Design of TRC barrel shells (Schneider et al. 2006).

## 2.4 Catenary curve in construction

Robert Hooke (1635-1703) was the first to discover that a hanging chain under the influence of self weight loading would form a catenary shape that was subject to pure tension. By inverting the chain in its current shape it was found that the shape would be in pure compression (Block et al., 2006). This shape displays the ‘line of action of the resultant compressive force’ that acts upon an erected arch (Harris, 2006): this is known as the thrust line of the arch.

Obviously, based on the additional weight applied, the thrust line will shift within the section of an arch. The structure will remain stable as long as the line of thrust remains within the boundaries of the structure (Huerta, 2005), as stated by the safe theorem developed by Heyman (1966). In a purely compressive state, should the line of thrust shift within the structure from the middle third to outside of it, then hinges will be formed within the structure due to the tensile forces created by this shift. If the line of thrust leaves the area of the middle third of the arch the tensile forces caused by this shift will cause cracks in the materials and thus reduce the structural soundness of the arch, as seen below in Figure 21.

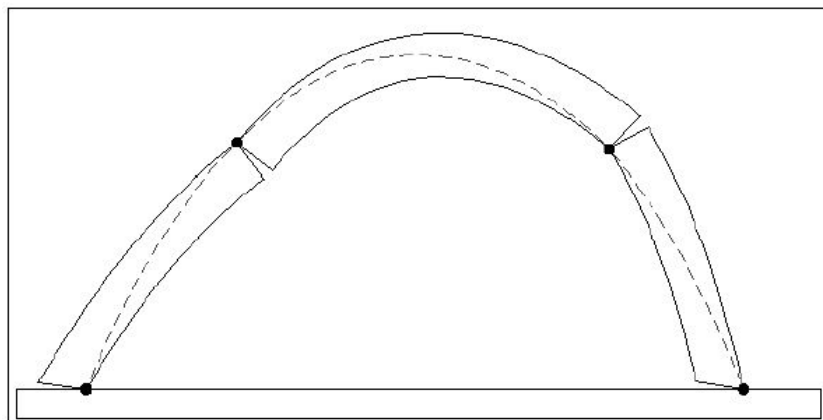


Figure 21: Example of a shifted thrust line forming hinges

Despite the formation of these hinges the structure will not collapse in these conditions according to the safe theorem developed by Heymans (1966).

This theorem was proven by Bulovic (2014), using the stress equation (taking compression as a negative):

$$\sigma = -\frac{P}{A} \pm \frac{Pe}{Z}$$

In this equation, it is assumed that the width of the arch is equal to a unit width.

Where

- P = Force
- A = Cross sectional area
- E = Eccentricity of force from centre line
- T = Thickness of arch
- Z = section modulus =  $\frac{bt^2}{6}$

If it is presumed that the tensile stress is zero in the case of the thrust line falling within the middle third then:

$$\sigma_t = \sigma_{bottom} = 0 = -\frac{P}{t} + \frac{6Pe}{t^2}$$

Once this is simplified and rearranged:

$$e = \frac{t}{6}$$

This accounts for one half of the middle third.

$$2e = \frac{t}{3}$$

Therefore proving that no tensile forces will occur within the middle third of an arch seen in Figure 20 below.

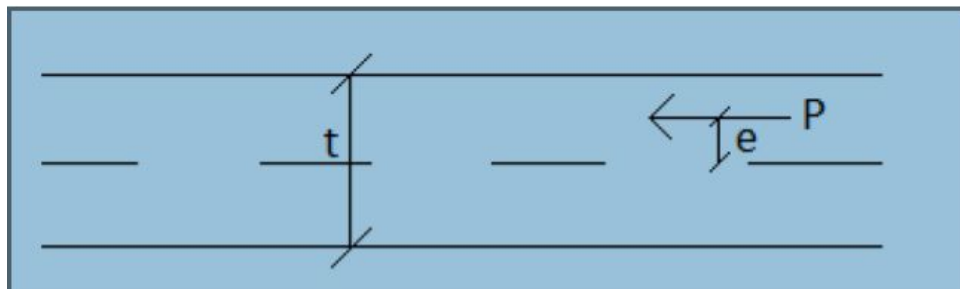


Figure 22:Diagram of arch used for proof (Bulovic, 2014)

This means that the optimal shape of an arch would be that of the catenary curve, as it allows for the line of thrust, displayed in Figure 22, to be contained in the middle third of the arch whilst using the least amount of materials.

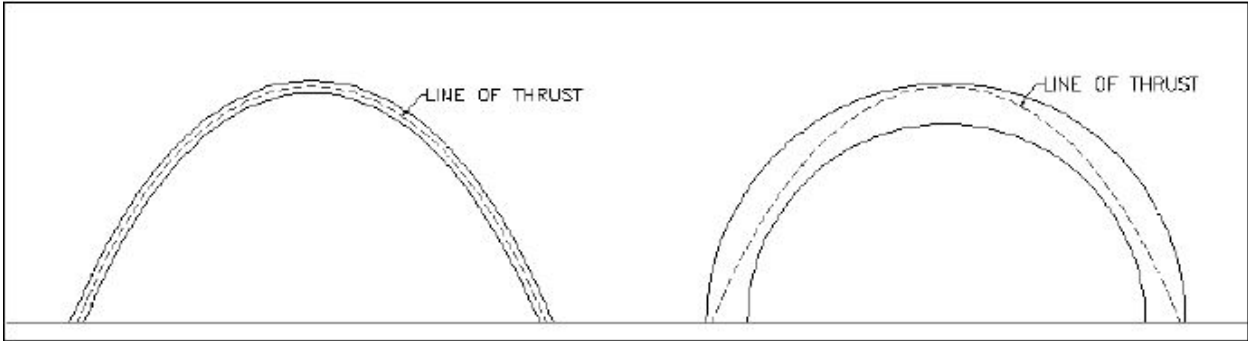


Figure 23: The catenary arch versus a semi circular arch

An example of an application of the catenary arch in structures is St Paul's Cathedral in England, which uses a catenary arch to support the lantern, but hides then by using false semi circular domes for aesthetic reasons.



Figure 24: St Pauls Cathedral

Another example of catenary arch structure is the Gateway arch in the USA.



Figure 25: Gateway Arch

In this research, the catenary curve will be used as a way of designing a structure that is purely in compression when it is under its self weight, which compliments the use of textile reinforcement in

construction as well as allowing for an aesthetic look to be achieved with the design (Block et al., 2006). With this design, the textile itself will activate only during periods in which the line of thrust moves away from the center third of the curve itself, so in case additional loads are applied to the structure, such as wind loads. The required catenary curve needs to be thick enough to accommodate its own self weight as well as additional loads, such as snow and wind. This is especially interesting, based on the transition to the use of natural fibres in TRC, which can support lower stresses than their non-biobased counterparts.

## 2.5 Schedule of requirements for the design of a (biobased) TRC pavilion

In order for the pavilion to be built in a manner that will end with a satisfactory result it is necessary to look at the specific requirements and address them individually.

Additional functional and technical requirements are established as a result of the research activities and will therefore be presented in the results chapter.

### 2.5.1 Functional requirements

The following list of functional requirements has been set up in collaboration with the in-company supervisor:

1. The pavilion must be suitable for the conversion to the use of biobased textiles, but due to the closure of the lab will be designed based on carbon textile properties.
2. The best biobased textile for the reinforcement must be determined by way of literature review, lab testing and MCA.
3. The design of the pavilion is based on a barrel vault, and it covers a surface of 4m x 4m.
4. A design of the foundations will not be done as the focus of the research is on the textile reinforcement.
5. The design of pavilion must favour the use of textile reinforcement and being realistic at the same time:
  - The use of a catenary curve as it reduces the amount of tensile forces in the structure.
  - Height and area of the pavilion that allow for real world use.
  - Smart use of materials and resources including reducing structural elements thickness.
  - Testing design in virtual analysis program(matlab) to determine required thickness.
6. Constructing the scale model of the pavilion according to the matlab output.
  - Ensuring that the curvature is correct along the entirety of the cross section.
  - The use of correct concrete mixture according to compression tests performed.

### 2.5.2 Technical requirements

The following technical requirements are established by looking into literature and regulations:

1. The testing of the design for the pavilion is realized using virtual analysis programs (MatLab, VCASLU and ) to determine the required thickness.
2. The design of the pavilion must handle self-weight, BSEN 1991-1-1.
3. The pavilion must be designed for additional loads e.g. snow loads (BSEN 1991-1-3), and wind loads (BSEN 1991-1-4)
4. The biobased textile material will be tested based on the following requirements:
  - Test the air content of the wet concrete mixture based on BSEN 12350-6:2009, Air Content.
  - Compressive test equipment based on BSEN 935-5:2012, Equipment for testing concrete.
  - Three point bending test based on EN 12390-6(2009), Testing hardened concrete.
  - Slump test, used to classify the workability of the concrete based on BSEN 12350-2:2009, Slump Test.
  - The density of the material used to calculate the self-weight of the concrete to be used in the pavilion design is verified using BSEN 12350-7:2009, Density.
  - The mixture design is based on the following regulations:
    - Setting times of concrete, BSEN 196-3:2016.
    - The use of Fly Ash, BSEN 450-1:2012.
    - The use of Silica Fume, BSEN 13263-1:2005+A1:2009
    - Admixtures (superplasticizer), BSEN 934-1:2008

### 2.5.3 Boundaries and limitation

Due to the closing of the labs at Scalda caused by the social distancing requirements mandated by the government for safety during the global pandemic (COVID-19) it became not feasible to carry out the majority of the planned experiments for the materials of the study. These being the uniaxial tension test, the pull out test as well as the three point bending test. Therefore it was necessary to expand the theoretical research to fill in the gaps in information.

This limitation has also determined the necessity to proceed with the design of the pavilion by using carbon textiles. The necessary laboratory tests to determine the structural properties of biobased TRC will be discussed in this report.

In this sense, this research represents a preparatory work to the further development of biobased TRC applications.

## 2.6 Selection of the textile for the design and construction of the pavilion

In this thesis multiple different textiles are being looked at and have varying characteristics that determine their effectiveness in the application of them as a reinforcement element that is to be applied. That means that it is necessary to set up a method in which the differing characteristics can be assessed in a manner that scales their impact on the design of the pavilion. In this research it was decided that a Multi Criteria Analysis would best suit the evaluation of the textiles as they all share similar characteristics but to varying degrees of effectiveness.

Tensile strength is a large factor in most reinforcements, as concrete has a low tensile strength in comparison to its compressive strength (Cauberg, et al. 2012). However, in the design of the pavilion used in this research the tensile forces are reduced to a level that is nearly negligible in terms of self weight and therefore this will have a lower weighting overall, namely 5% as it will have the least effect on the design of the pavilion

Cost will have a large impact on the outcome of the design of the pavilion due to the fact that in the construction industry costs play a large role in whether the bid for a project is won or not, it is also one of the factors that varies the most. This comparison is purely based on the cost of the textile reinforcement materials and not the total cost of a project e.g including concrete. Therefore it was decided that it would carry the highest weighting overall with a 30%.

Workability is a large part of the endorsement of textile reinforcement as it allows for the use of concrete to be similar to what it used to be referred to as, liquid stone. With the workability of most of the textiles being of a similar nature, as they are all pliable with similar penetration of concrete between, it was decided that this would have a lower weighting of 5% as it will not have a large impact on the score.

Carbon footprint is one of the main factors used when measuring the environmental impact of an activity or product and with this being a part of the postdoc of Dr G. Scuderi, which is focused on creating new materials or technologies able to improve the current construction climate with the use of biobased materials in conjunction with concrete. It was thus deemed necessary to give this criteria the highest weighting overall with 30%.

The self weight and or density of the materials themselves will have an impact on the design of the pavilion or any construction they are used in as it affects the overall loads and forces that will be experienced by the structure and with the range of the densities of textiles being examined it is necessary to take it into account. But with the densities of the textiles being very light in comparison with the other materials being used in the design of the pavilion and therefore receives a lower weighting of 10%.

Another environmentally impactful criteria being looked at is the energy consumption required to produce and or use the textiles. It is indirectly related to the use of the textiles and thus will be weighted lower than that of the carbon footprint at 15%.

Compatibility of the materials with the concrete is another factor that will affect the quality of the project as incompatibility could lead to a shorter life span. As this is a qualitative criteria based on observations made of the pretreatments of the biobased fibres, the observation the glass fibres lose their compatibility overtime when used in concrete (Hall and Ghali,2000) and carbon fibres require an epoxy treatment to reduce slipping (Williams Portal, N., 2015). This criteria will have a weighting of 5% as it will require more tests such as e.g pull out tests of all the materials to have a better comparison.

In this MCA each column represents a certain characteristic of the textiles that are being examined and compared. Each of these characteristics is given a weighting that represents the importance of said characteristic. These weighting are then multiplied with the score given to each textile which is given out of ten, with ten being the best possible solution, 0 being the worst, and the rest being scale between the two based on information found in literature review. The overall score is then added up by combining all of the resultant scores in a row which will give an overall score out of ten per textile material.

## 3. Methodology

To be able to obtain the answer to the final question and design the pavilion, the methodology has to be defined. Below the different sections of the thesis are broken down into their separate parts and discussed as to their purpose and what will take place.

### 3.1 Desk research

#### 3.1.1 Literature review

In the research proposal the following part of the thesis has been taken care of. During the design phase of the pavilion, if it is necessary, more information may be researched in accordance with the requirements of the design and structural reliability. This information will be added to the final report as theoretical background at a later stage. Therefore this part allows for the answering of some of the research sub-questions.

#### 3.1.2 Multi criteria analysis

There are several different materials that are being looked at in this thesis with multiple characteristics and it is therefore necessary to perform a multi criteria analysis. The multi criteria analysis will be done to evaluate which variant is the most feasible to be used in the next stage of the research, that being in the design of the pavilion. Therefore the multi criteria analysis will take into account all the characteristics that will most affect the design of the pavilion. Examples of the factors that will be looked at in this multi criteria analysis will be tensile strength, cost, ease(workability) and carbon footprint.

It is worth to mention that in origin the MCA should have also included results verified through laboratory testing. However, due to the limitations previously mentioned the MCA will include information derived only from literature sources.

## 3.2 Experiments

In this research, varying standards are used to determine the workability, air content, density and mechanical properties of the fresh concrete namely: EN-12350-5 (2010) for the concrete, EN-12350-2 (2009) for the slump test, EN-12350-7 (2009) for the air content, and EN-12350-6 (2009) for the density.

### 3.2.1 Concrete matrix tests

#### 3.2.1.1 Workability

Following EN-12350-2 (2009), the tests procedure, also known as the slump test, can be explained in a number of steps:

1. All the ingredients required to make the concrete are placed into an automatic mixer and are thoroughly mixed. This mixture is then placed in an Abrams cone in 3 layers with 25 pokes of a stick done between every layer.
2. The Abrams cone is then removed directly upwards to prevent jostling of the mixture. The mixture is then subject to its own self-weight causing it to slump. The Abrams cone is then placed beside the pile of concrete to be used as a reference point.
3. After the fresh has finished settling the distance between the height of the Abrams cone and the height of the concrete pile is measured to determine the workability of the concrete with the chart seen below.

► Consistentieklassen (op te geven door aannemer)			
Aanduiding	Verdichtingsmaat c	Zetmaat (mm) h	Schudmaat (mm)
Droog	C0	≥ 1,46	
Aardvochtig	C1	1,45–1,26	S1 (30–40)
Halfplastisch	C2	(1,25–1,11)	S2 50–90
Plastisch	C3	(1,10–1,04)	S3 100–150
Zeer plastisch		S4 (160–210)	F4 490–550
Vloeibaar		S5 (≥ 220)	F5 560–620
Zeer vloeibaar			F6** (≥ 630)

\* Voor schudmaat aangepaste kegel H=200 mm gebruiken (1/3 x schudmaat).  
 \*\* Voor zelfverdichtend beton vloeimaat en stabiliteit volgens BNL 1801 en C18-voorbereiding 93.

Figure 26: Chart for slump test



Figure 27:Mixing of the concrete



Figure 28: Abrams cone with concrete pile adjacent

This method is used to determine the workability of the concrete that will be used in the design of the pavilion. After the slump flow test the mixture was placed back with the rest of the mixture to be further tested and then placed into cubic moulds of 150mm by 150mm. This is where it was then left to set for at least 24hrs before removed from the mould and placed in a water bath for a further 6 and 27 days. These cubes will then be used in the mechanical properties testing.

#### 3.2.1.2 Air content

Following the EN-12350-7 (2009) procedure for the testing of the air content of a concrete mixture can be explained in the few steps that follow.

1. The container seen in the figure below is placed on a vibrating table. This container is then filled with the same mixture mentioned in the previous test. This container is then vibrated and filled until the concrete fills the container to the edge. The vibrating is used to cause the concrete to settle.
2. The container then has its lid placed on it and sealed so that it is airtight. Water is then poured in through the holes in the lid to displace any excess air trapped on the surface of the concrete that could affect the test results. These holes are then sealed as well and the container is pressurized.
3. Once the container is fully pressurized a valve is released giving the actual value in terms of percentage of the concrete is air thus giving the air content. This mixture is then placed back into the original mixture which will then be used in the following tests.



Figure 29: Air content testing container

### 3.2.1.3 Density

Following EN-12350-6 (2009) procedure for the testing of the density of the concrete density. The following steps are required.

1. The cubic mould is filled with the previously discussed concrete which is then vibrated to ensure settlement and compaction this block is then allowed to set over a 24 hr period where it is then removed from the mould.
2. This concrete is then placed into a water bath for a further 6 and 27 days to set to its maximum compressive strength after a total of 7 and 28 days. This cube is then measured on all sides to determine its volume. The cube is then weighed.
3. This weight is then used to calculate the density of the concrete with the equation:

$$Density = \frac{Weight}{Volume}$$

### 3.2.1.4 Compressive strength test

The mechanical strength tests are required to be performed on the concrete to determine the compressive strength of the concrete mixture. These are done according to EN 12390-3(2009) procedures. The steps followed are as follows.

1. The concrete cubes have been removed from their moulds and have been aged for a length of 7 and 28 days with three in each category. These cubes are then measured to ensure that they are according to EN 12390-1(2012) for dimensions. A deviation of 6% is allowed.
2. These cubes are then placed into a press. The press will apply pressure to the cube increasingly until the cube cracks and/or breaks. The press will then display the maximum force applied.
3. This value is then recorded and divided by the pressure zone(area of the face). This will give a compressive strength in terms of N/mm<sup>2</sup>.



Figure 30: Compression test of concrete cubes

### 3.2.2 Textile reinforced concrete tests

#### 3.2.2.1 Construction of the TRC specimens

The concrete is used to fill the mould built according to the required specifications set out in EN 12390-6(2009). This mould dimensions can be seen in the figure below.

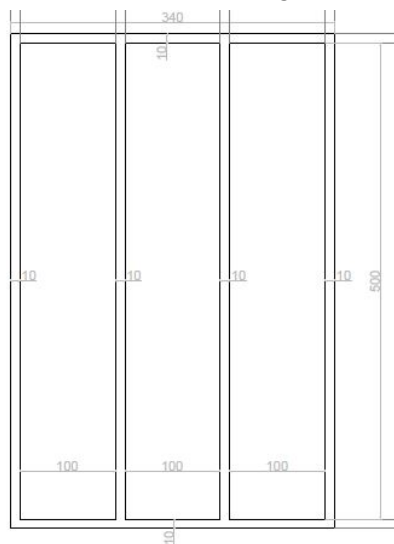


Figure 31: Dimensions of mould used

This mould is used in order to produce three sheets of TRC of the dimensions 500mm by 100mm. The process in which this mould is filled is as follows.

1. Fill the first layer of the mould which is 10mm in height. This is done for all three sections of the mould for each sheet.
2. A layer of textile reinforcement is then laid on top of these three sections and with the use of a vibrating table or a roller is half submerged in the concrete. The textile reinforcement is required to be laid with the direction of the fibres being parallel and perpendicular to the length of the sheet.

3. The second layer of the mould is attached which matches the first layer but has no bottom. This allows for the textile reinforcement to pass through the sheets completely and parallel without the need to trim the sheets afterwards.
4. The second layer of concrete is then added on top of the first layer to add another 10mm to the concrete sheet.
5. The entire mould is then vibrated to ensure penetration of concrete through the gaps in the textile.
6. These are then left to set for 24 hours before being removed and placed in a water bath for a further 27 days.



Figures 32 and 33: The two different layers of the mould empty and filled respectively



Figure 34: Single sheet of TRC removed from mould

### 3.2.2.2 Uniaxial tensile test

Once the TRC sheets have set for the required 28 days it is now necessary to test them. This is done as a uniaxial test to determine the load bearing behavior of the specimens made of TRC. The following steps are followed according to Rilem TC 232-TDT.

1. The sheet is measured to ensure it complies with the minimum requirements of EN 12390-6(2009). It is then placed into the tension machine that clamps either side, leaving a minimum length of 200mm in the center for the measuring range as displayed in the figure below. This machine can be any machine as long as it is able to provide the necessary loads and movement. It is required to have an accuracy of extensometers according to ISO 9513 and a force measuring system according to ISO 7500-1.
2. Deformation measuring equipment is then attached to the sheet before any loads are applied.

3. The tensile tests are then carried out in deformation controlled mode by crosshead displacement at a strain rate of  $2 \times 10^{-3}/\text{min}$ . The test is terminated at a loss of at least 70 % of the maximum load.
4. The loads and deformations are then recorded and utilised to determine the stress-strain relation of the TRC. For the strain the deformations are recorded, averaged and then related to the measuring length of the specimen. The stress is determined from the force applied to the specimen and the cross sectional area of the specimen.

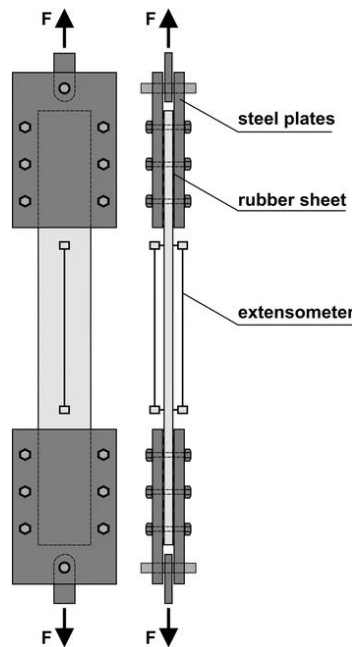


Figure 35: Example of TRC sheet in tension machine

### 3.2.2.3 Three point bending test

Another mechanical strength test that is required when dealing with textile reinforced concrete is the three point bending test according to the EN 12390-6(2009) procedure. These tests are carried out as follows.

1. The thorough mixing of the same concrete mixture. This mixture is then placed into a sheet mould as seen below. This mould has 2 layers, this is done so that the textile can be placed precise in the center of the sheet. This mould has the minimum dimensions of 60mm by 500mm and minimum thickness of 6mm.
2. This concrete mixture is then left to set for 24 hrs before it is demoulded and placed in the water bath for a further 27 days to set to full strength. And is then removed.
3. These sheets are then placed in the three point bending test machine individually and pressure is applied until cracking forms. These results are then recorded. This gives the elastic modulus, stress and deformation of the sheet. A maximum of 15% deviation is allowed between similar specimens.



Figure 36: Three point bending test of concrete sheet

### 3.2.3 Construction and testing of a scale model for the TRC pavilion

The construction of a scale model needs to be accurate to the design to ensure that the results best represent the real situation. It is also necessary that the model be small enough to be built in the lab as a precast structure to reduce chances of imperfections. Therefore the following steps will be followed.

1. A mould for the model will be built at a scale of 1:5. This mould will be built according to the outer measurements of the pavilion, for the first part, and laid so that the opening at the bottom is facing up. It will have edges of 1cm thick due to the scaling of the pavilion.
2. Concrete will then be filled into the mould up to 1cm in thickness. The textile reinforcement is then laid on the surface of the wet concrete.
3. The second part of the mould is then attached which is the 1cm left of the thickness. This is then filled as well with a further 1cm of concrete.
4. The last part of the mould is then applied which is essentially a lid that follows the shape of the inner curve of the pavilion. This is done to ensure that whilst the concrete is setting it keeps an even distribution of 2cm throughout.
5. This is then left to set for 24 hours. The mould is then removed and the pavilion is left to cure for a further 27 days.

Once the pavilion has been cured for a total of 28 days it is then possible to start testing it to determine if it can handle the loads such as self weight, snow loads and wind loads. The following steps were taken when applying the loads on to the pavilion.

1. The pavilion is placed on a flat stable surface that is easily accessible from all directions. And secured to arrest movement at the bases.
2. The dimensions are then measured throughout the entire pavilion.
3. The loads are then placed on the pavilion incrementally until the maximum snow load scaled to the pavilion is reached. These loads are applied in terms of weights.
4. In terms of the wind load a shaking table is used as a form of increasing the horizontal forces on the pavilion.
5. The measurements of the pavilion are then taken again to determine the displacement of the pavilion due to the loads applied. Checks for cracking will be done as well and compared with the allowable results found in the literature review.

### 3.3 Design of pavilion

Once the favourable material has been found using the desk research, MCA and experiments, it is necessary to design the pavilion in a manner that best suits the characteristics of the textile chosen. Therefore in this research a pavilion with a catenary curve in one direction will be designed with the parameters of a 4m by 4m. The other direction will be flat and follow the curve of the other plane, similar to that of a barrel vault. This pavilion will be designed to accommodate the loads of self weight, wind load and snow load to ensure that it is safe to use. The reason that this design was chosen is that it will reduce the amount of tension forces found in the construction as textile reinforcements are not as strong as standard steel rebar.

This design will then be modeled using the program matlab to determine whether the chosen thickness used in the design is able to achieve a safe pavilion(vault).

Matlab is a maths based program that allows the user to calculate maths equations with the advantage of visual outputs to determine the best solution. This is done with the use of Finite Element Analysis(FEA). FEA is the analysis of a material or object with the use of the Finite Element Method(FEM). This system divides a larger object or material into smaller and simpler parts that are possible to calculate. These are called finite elements. This is achieved by converting the object or material into a mesh as seen below. These are then solved with the use of Partial Differential Equations(PDEs).

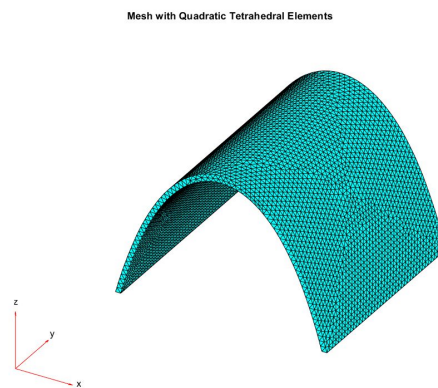


Figure 37: Mesh grid of pavilion

In Matlab there are five specific steps that are taken to achieve this form of analysis on the structure. First it is necessary to define the geometry of the object that is to be analysed. In the case of this thesis, (the object being the pavilion) the object was first modelled in another software, AutoCAD, and then exported as a stereolithography file, a file format used in 3D modeling softwares. This file is then able to be imported into Matlab.

Secondly it is necessary to define the PDE coefficients required for the analysis. There are multiple different types of PDEs which are used for different types of analysis. In this thesis the use of the Eigenvalue PDE will be used as its application in Matlab is for structural mode shapes. This equation can be seen below.

$$-\nabla \cdot (c \otimes \nabla u) + au = \lambda du$$

The coefficients found in this equation such as a, c or d can represent various different things, such as coupled PDEs, the functions of speed, time or direction allowing for nonlinear problems, or they could represent complex numbers.

Thirdly the boundary conditions need to be defined. Within the Matlab toolbox, two types of boundary conditions can be defined, Dirichlet which is used in civil engineering on structures with supports, or Neumann which is more commonly used in thermodynamics. Dirichlet was decided as the correct choice. It is now necessary to mesh the geometry. Matlab uses tetrahedral elements. This can be seen in the figure above.

It is now possible to solve the problems of the object and then visualise the results using the functions found in Matlab and its toolboxes. Examples of the outputs of results that are used in this thesis include, deformation, stress found, and strain.

In the following paragraphs, the methods are presented in further details.

### 3.3.1 Shape finding

The shape of the pavilion is influenced by multiple factors such as environmental, stability, efficiency and usable space. In terms of environmental reasoning, the ability to reduce the amount of construction materials required is seen as a positive factor, as all construction materials have a certain carbon footprint. For example, cement has a ratio of 1:1 in terms of CO<sub>2</sub> produced to cement used. This leads to the search for a design that allows for the use of less materials.

A catenary curve allows certain strengths with less material used, due to its shape which follows the line of thrust of an arch. This means that in terms of stability, a catenary curve allows to express the self-weight of the structure as pure compressive forces. This allows the use of construction materials which perform best in compression, such as stones, bricks or concrete. Since the structural behaviour of the construction materials can be optimized, it is possible to reduce the thickness required of the arch without hindering the stability of the structure.

The catenary curve is expressed with the equation.

$$y = a \cosh\left(\frac{x}{a}\right)$$

With 'a' being the shape factor of the equation determining the shape and size of the curve as seen below in figure 38 , and x and y representing the horizontal and vertical coordinates.

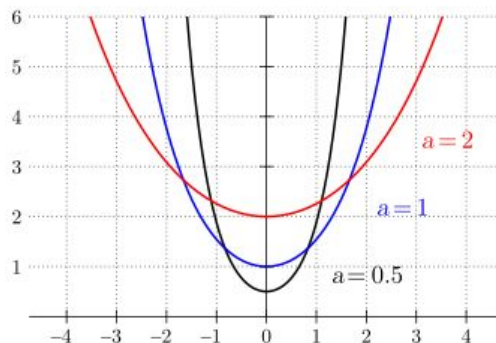


Figure 38: different types of catenary curves.

By using an ‘a’ factor equal to 1, it was possible to optimise the gradients of the sides of the pavilion to maximise space whilst keeping the ceiling lower to reduce the amount of material required for construction.

From these assumptions, it was possible to derive the pavilions shape necessary to cover an area of 4m by 4m, seen below in figure 39, still allowing for accessibility.

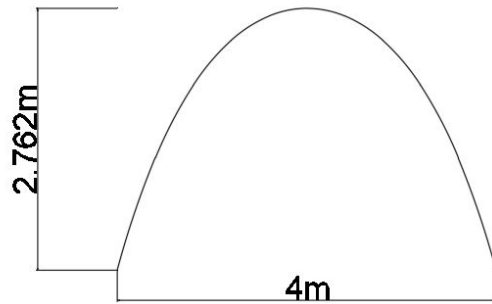


Figure 39: Catenary curve

### 3.3.2 Load calculations

#### 3.3.2.1 Structural self-weight

The structural own weight is given by the weight of the concrete which for CEM I 52.5 R is equivalent to a specific weight of 25 kN / m<sup>3</sup>. This value, multiplied by the thickness of the shell and by half of the length of the structure, gives us the dead load which acts in the negative z direction.

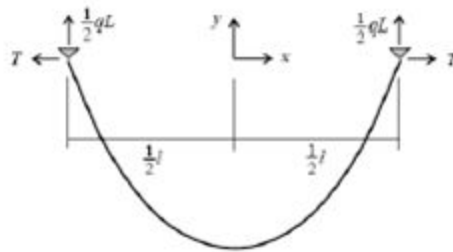


Figure 40: Loads of a curve

$$q_{self\ weight} = 25 \cdot 0.1 \cdot 7.252 = 18.13 \frac{KN}{m}$$

#### 3.3.2.2 Snow load

Snow loads have a significant effect on shell structures as they add to the overall weight of the structure.

This use of BSEN 1991-1-3 is used to obtain the snow loads that will be experienced by the pavilion. The equation used for this calculation is:

$$s = \mu_i \cdot C_e \cdot C_t \cdot s_k$$

Where :

$s_k$  = Characteristic value for the snow load = 0.7kN/m<sup>2</sup>(for the whole of the Netherlands)

$C_e$  = Exposure coefficient = 1 (assumed for normal topography)

$C_t$  = Thermal coefficient = 1.0

$\mu_i$  = Snow load shape coefficients

The Eurocode provides snow load coefficients for cylindrical roofs as shown below.

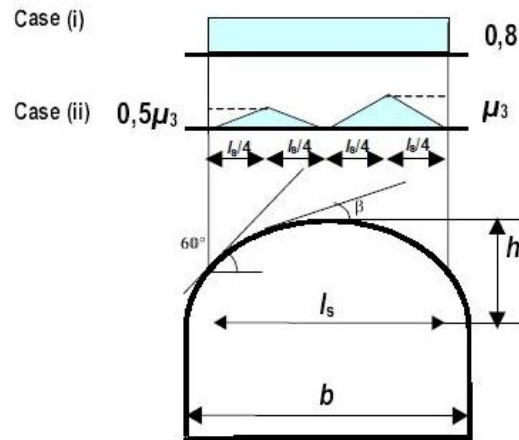


Figure 41: Snow load cases for cylindrical roofs

The first case(case(i)) is for an undrift load arrangement which is representative of an evenly distributed snow load on the structure. The second case(case(ii)) is for drifted load arrangements as a result of the rearrangement of the snow(e.g due to wind)

$$\text{For } \beta \leq 60^\circ, \mu_1 = 0.8$$

$$\mu_3 = 0.2 + 10 \cdot \frac{h}{l} \quad (\mu_3 \leq 2.0)$$

$$\text{For } \beta > 60^\circ, \mu_1 = \mu_3 = 0$$

Therefore for case(i):

$$s = 0.8 \cdot 1 \cdot 1 \cdot 0.7 = 0.56 \text{ KN/m}^2$$

And for case(ii):

$$\mu_3 = \left( 0.2 + 10 \cdot \frac{2.762}{4} \right) = 7.105$$

Due to restrictions mentioned above the values taken case(ii) will be 2 and 1 respectively.

$$s(\mu_3) = 2 \cdot 1 \cdot 1 \cdot 0.7 = 1.4 \text{ KN/m}^2$$

$$s(0.5\mu_3) = 2 \cdot 0.5 \cdot 1 \cdot 1 \cdot 0.7 = 0.7 \text{ KN/m}^2$$

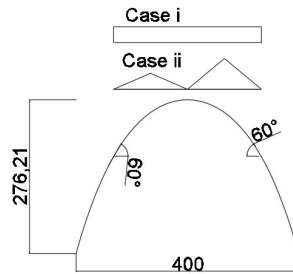


Figure 42: Snow load cases on pavilion

The loads applied in case(ii) using the scheme shown below. The original loads are of a non uniform nature and were therefore approximated as smaller uniform loads for easier modeling.

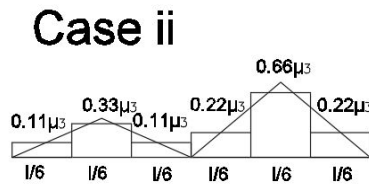


Figure 43: Case(ii) approximations

### 3.3.2.3 Wind load

The wind loads experienced on a structure are calculated in the form of pressure coefficients. These coefficients act over the whole surface of the structure, in this case being the shell pavilion. The wind pressures are calculated based on the size and shape of the structure they are acting upon.

These calculations begin with the calculation of the wind velocity in the area the structure is being constructed in. In the equation below the constants  $c_{dir}$  and  $c_{season}$  are the directional and seasonal constants respectively, which both have a recommended value of 1.



Figure 44 : Zones of the Netherlands

The basic wind velocity value is denoted as  $v_{b,0}$  and according to BSEN 1991-1-4 for region II in the Netherlands, displayed in figure 44, this value is equal to 27 m/s.

$$v_b = c_{dir} \cdot c_{season} \cdot v_{b,0}$$

$$v_b = 27 \text{ m/s}$$

Once this value has been found it is possible to calculate the peak velocity pressure with the formula found in BSEN 1991-1-4.

$$q_p(z) = \left[ 1 + 7 \cdot I_v(z) \right] \cdot \frac{1}{2} \cdot \rho \cdot v_m^2(z) = c_e(z) \cdot q_b$$

Where  $c_e(z)$  is found using the figure 45 provided by the Eurocode(below). This value is found using terrain category II.

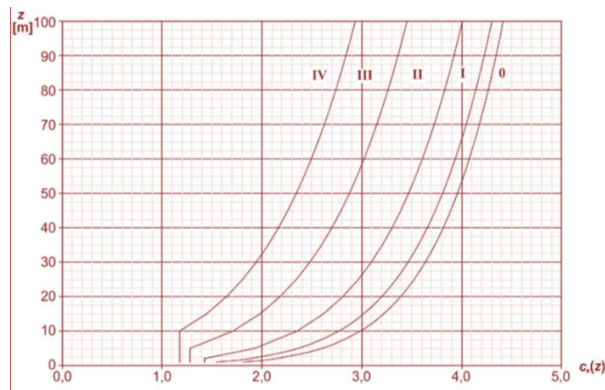


Figure 45: Illustrations of the exposure factor  $c_e(z)$

And  $q_b$  is obtained using air density( $\rho$ ) and the basic wind velocity. The air density has a recommended value of 1.25kg/m<sup>3</sup>. The calculation can be found below.

$$q_b = \frac{1}{2} \cdot \rho \cdot v_b^2$$

This gives a final equation of:

$$q_p(z) = 1.4 \cdot \frac{1}{2} \cdot 1.25 \cdot 27^2$$

$$q_p(z) = 0.637 \text{ KN/m}^2$$

*(Cpe) External pressure coefficient*

The external pressure coefficient depends on the amount of the air and therefore on the geometry of the structure. The diagram provided below for rectangular-based vaulted roofs is used for the structure under consideration.

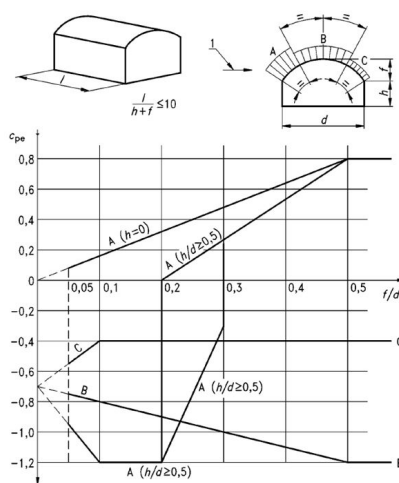


Figure 46: Cpe coefficients

$$\frac{f}{d} = \frac{2.762}{4} = 0.69$$

From this the following figures are obtained:

$$C_{pe}(A) = 0.8$$

$$C_{pe}(B) = -1.2$$

$$C_{pe}(C) = -0.4$$

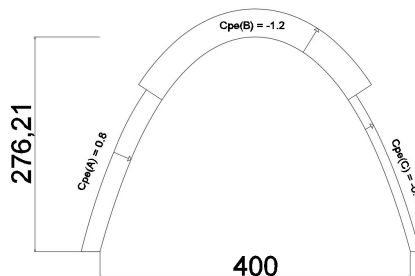


Figure 47: Applied Cpe coefficients

These values are then used in the equation:

$$w_e = q_p(z) \cdot c_{pe}$$

Which will give the results as to how the wind load will affect the pavilion in the specific regions it is being applied.

$$w_{e(A)} = 0.637 \cdot 0.8 = 0.5096 \text{ KN/m}^2$$

$$w_{e(B)} = 0.637 \cdot -1.2 = -0.7644 \text{ KN/m}^2$$

$$w_{e(C)} = 0.637 \cdot -0.4 = -0.2548 \text{ KN/m}^2$$

### Internal pressures

Due to the pavilions interior being exposed by the opening on two of the sides, it is necessary to calculate the internal pressure. This is achieved with the following equation.

$$w_i = q_p(z) \cdot c_{pi}$$

With  $q_p(z)$  known already from the previous equation that leaves just  $c_{pi}$  to be found in order to calculate the internal pressure experienced by the pavilion. This is done with the following steps.

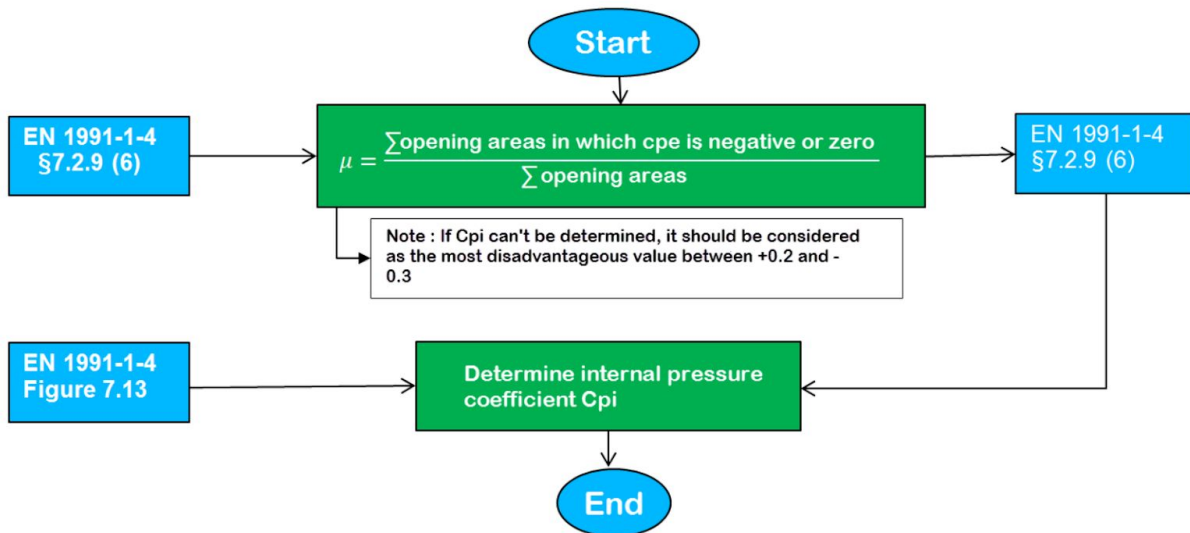


Figure 48: Cpi calculation flow chart

Determining the  $c_{pi}$  comes from interpolating from the figure below.

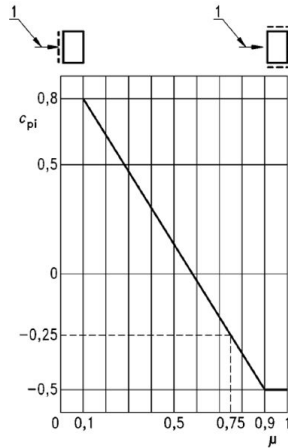


Figure 49: Cpi coefficient

This case being :

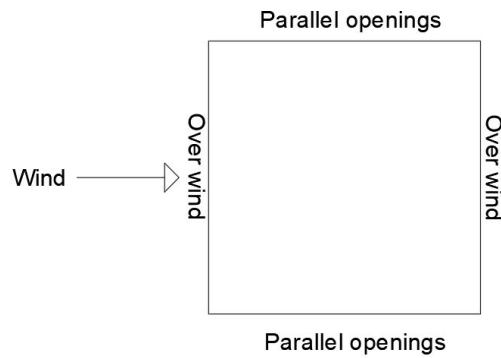


Figure 50: wind direction in relation to openings

The only openings of the pavilion are parallel with the direction of the wind and there for it is determined that the  $\mu$  value is equal to 1.

From this it was found that the  $c_{pi}$  coefficient value was equal to -0.5.

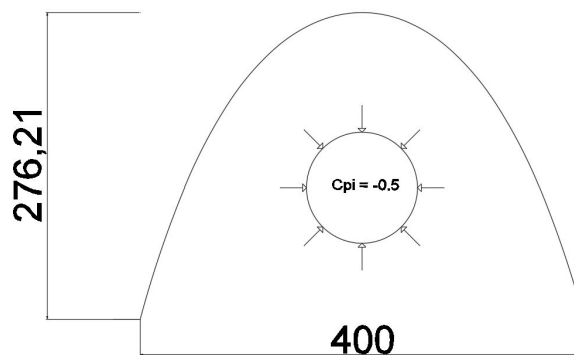


Figure 51: Internal pressure coefficient

The  $w_i$  internal pressure value will then be:

$$w_i = 0.637 \cdot -0.5$$

$$w_i = -0.3185 \text{ KN/m}^2$$

### The NET pressures

The net pressures exerted on the structure are the sum of the different pressures in each region, said being A, B and C, to get a total pressure acting in one direction for each region. If acting toward the pavilions surface it will be taken as positive and away will be regarded as negative, as seen in example below.

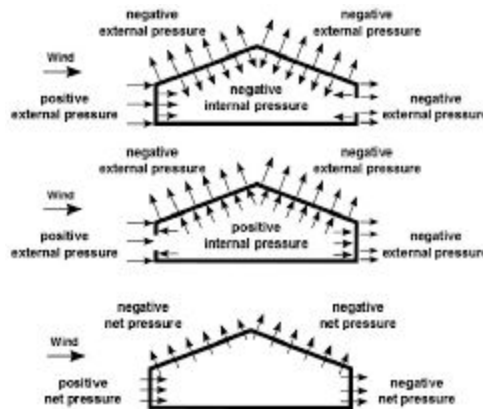


Figure 52: Net wind pressure

In the case of the pavilion it is:

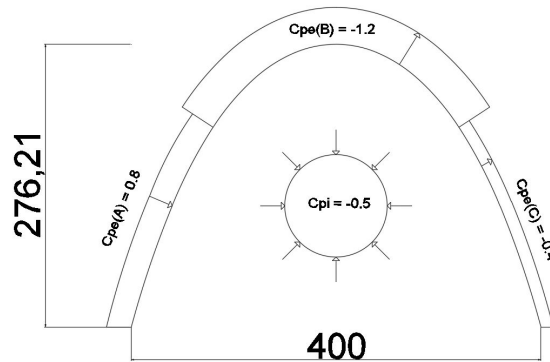


Figure 53: Internal and external coefficients

From this the  $c_{pn}$  (net coefficient) can be calculated:

$$c_{pn(A)} = 0.8 + 0.5 = 1.3$$

$$c_{pn(B)} = -1.2 + 0.5 = -0.7$$

$$c_{pn(C)} = -0.4 + 0.5 = 0.1$$

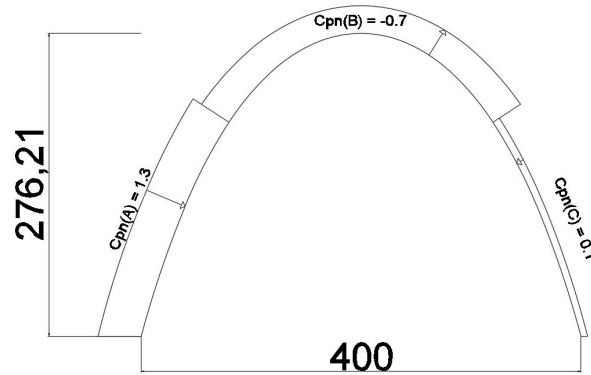


Figure 54: Net pressure coefficients

Therefore the net pressures exerted on the pavilion are:

$$w_{n(A)} = 0.637 \cdot 1.3 = 0.8281 \text{ KN/m}^2$$

$$w_{n(B)} = 0.637 \cdot -0.7 = -0.4459 \text{ KN/m}^2$$

$$w_{n(C)} = 0.637 \cdot 0.1 = 0.0637 \text{ KN/m}^2$$

The action of the longitudinal wind is not analyzed, as it is only acting upon the surface as a friction load and on the thickness of the pavilions walls. In view of the fact that the structure has a very high rigidity in that direction, the tangential friction component is also not significant.

### 3.3.3 Buckling checks

The Euler buckling equation is used for axially loaded elements under compression. This check is more commonly known as the critical buckling loads of compression elements. These formulas are based on columns and pillars but Timoshenko and Gere (1963) suggest that these equations can be further utilised for more complex structure, for example arches. The most common of these equations are:

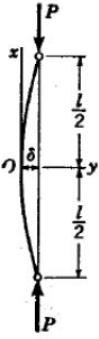
End condition	Description	Equation
	<p>Both ends are connected with a pin joint and translation in the axial direct is allowed. Lateral translation however is not. The ends have free rotation.</p>	$P_{cr} = \frac{\pi^2 EI}{l^2}$
	<p>Both ends are fixed and thus do not allow rotational and lateral translation. Axial translation however is allowed.</p>	$P_{cr} = \frac{4\pi^2 EI}{l^2}$

Table 3: Euler buckling equations

### *Buckling of a curved bar*

According to Timoshenko and Gere, (1963), the critical buckling load of a curved bar can best be described using the following equation.

$$\frac{d^2w}{d\theta^2} + w = -\frac{R^2 S w}{EI}$$

Where:  $S = qR$

- $q$  = Uniformly distributed load
- $w$  = Radial displacement towards the centre
- $R$  = Total length of curve
- $E$  = Modulus of elasticity
- $I$  = Moment of inertia of the section
- $\theta$  = Variable length of curve

This equation can then be manipulated to find a solution by using calculus, this then gives the equation for the critical buckling load of a uniformly compressed circular arch (Timoshenko & Gere, 1963).

$$q_{cr} = \frac{EI}{R^3} \left( \frac{\pi^2}{\alpha^2} - 1 \right)$$

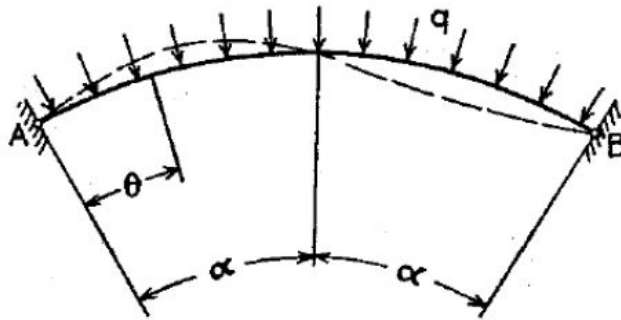


Figure 55: Curved arch with a uniform load

Alternatively, the critical buckling load can be determined with the use of an effective length factor ( $\beta$ ) to the original Euler equations. This allows for a simplification of determining the critical buckling load by increasing or decreasing the size of the effective length considered in the equation. By increasing the effective length, the critical buckling load will be reduced. A reduction of the critical length will increase the critical buckling resistance. This factor can be calculated with the equation below.

$$\beta = \frac{s_k}{s}$$

The critical buckling load of an arch at its supports can be calculated using the following formula.

$$P_{cr} = \left( \frac{\pi}{\beta s} \right)^2 EI_y$$

Where:  $\beta$  = Effective buckling length factor

E = Modulus of elasticity of the arch material

$I_y$  = Second moment of inertia about the weak axis of section

The coefficient ( $\beta$ ) for various types of arches have been plotted for various conditions. These are plotted as a relationship between ( $\beta$ ) and the ratio of rise to span ( $h/l$ ) or the arch (German Building and Civil Engineering Standards Committee & German Committee for Structural Steelwork, 1990). Below can be seen the plotting of the different ( $\beta$ ) for different situations.

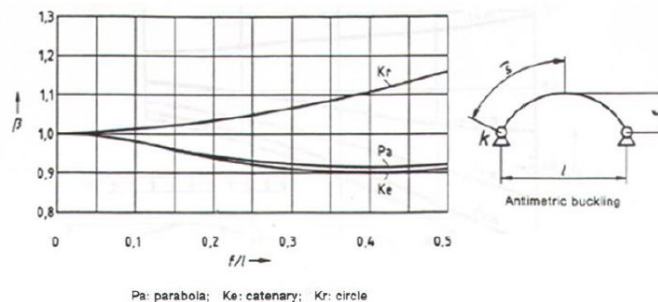


Figure 56: 2 joint arch buckling coefficients

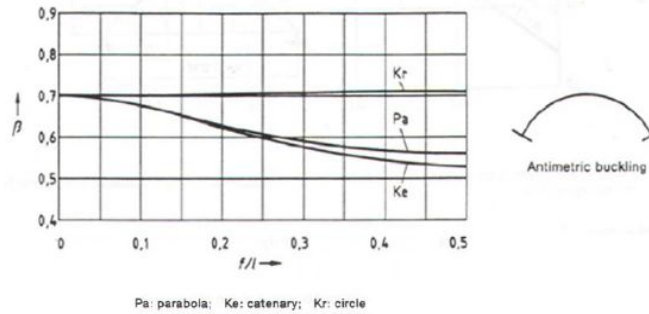


Figure 57: Fixed support buckling coefficients

*Buckling load of catenary arch*

With further calculation and applying the theory of buckling of arches, the critical uniform pressure of a catenary arch can be calculated with the equation (Timoshenko & Gere, 1963):

$$q_{cr} = \gamma_4 \frac{EI}{R^3}$$

The values for the constant  $\gamma_4$  in this situation are based on the number of hinges found in the arch as well as the ratio of the rise of the arch to its span. This is displayed in the table found below.

h/l	No Hinges	Two Hinges
0.1	59.4	28.4
0.2	96.4	43.2
0.3	112	41.9
0.4	92.3	35.4
0.5	80.7	27.4
1	27.8	7.06

Table 4: Values of the constant ( $\gamma_4$ ) for catenary arches of constant cross-section with load uniformly distributed along the arch's axis (Timoshenko & Gere, 1963).

Another buckling check that is done is the critical pressure of an arch. This load is calculated to determine the maximum pressure that can be experienced by the structure whilst still resisting buckling. This check is based on the thickness of the structure and the radius of the curve of the pavilion.

An application of a knockdown factor is used in this equation. This factor is used as a reduction factor to account for the imperfections that could be found in the structure once it is actually built.

$$P_{crit} = \frac{2}{\sqrt{3(1-\nu^2)}} \cdot E \left( \frac{t}{a} \right)$$

$\nu$  = Poisson's modulus

$E$  = elastic modulus

$t$  = thickness

$a$  = radius, variable in this case

**Young's modulus And Poisson's Ratio For Some Materials**

Materials	Young's Modulus	Poisson's Ratio
Steel	2.1e5	0.3
Cast Iron	1.20e5	0.28
Wrought Iron	1.90e5	0.3
Aluminium	0.70e5	0.35
Aluminium Alloy	0.75e5	0.33
Brass	1.10e5	0.34
Bronze	1.20e5	0.34
Copper	1.20e5	0.34
Copper Alloy	1.25e5	0.33
Magnesium	0.45e5	0.35
Titanium	1.10e5	0.33
Glass	0.60e5	0.22
Rubber	50	0.49
Concrete	0.25e5	0.15

Figure 58: examples of Young's modulus and Poisson's ratios

### 3.3.4 Crack control in the arch.

Cracking occurs due to the tensile stresses being loaded onto the concrete. These cracks occur when the force exceeds the maximum tensile strength of the material and it is thus necessary to add the reinforcement to increase this tensile strength.

The calculation of crack widths is done using the concept of 'fracture energy regularisation' (Peerdeman, 2008). With this theory, it can be assumed that there is the one crack in each element, the width  $w$  of which depends on the equivalent length on the element or crack bandwidth  $h$ .

$$\varepsilon = \frac{w}{h} \Rightarrow w = \varepsilon * h$$

In the equation above,  $\varepsilon$  is the strain found in the element,  $h$  is the length of the element and  $w$  is the crack width to be calculated. The maximum strains will be extracted from the results from the Matlab model and the corresponding crack widths will be calculated in that element. Now the crack opening criteria has to be established to check the structure for undesirable cracks. This criterion is established based on the recommendation of AFGC, the widely accepted French guidelines for concrete. The recommendations provided by AFGC state the following values for crack widths:

– 0.3 mm for highly detrimental cracking

- 0.2 mm for detrimental cracking
- 0.1 mm for normal cracking

### 3.3.5 Stability check

The stability of the arch is dependent on the thrust line of the arch and its shift due to the forces applied and the displacement of the arch itself. In order to keep the arch stable and to ensure that no hinges are formed in the arch the thrust line must remain within the middle 1/3 of the thickness as seen below.

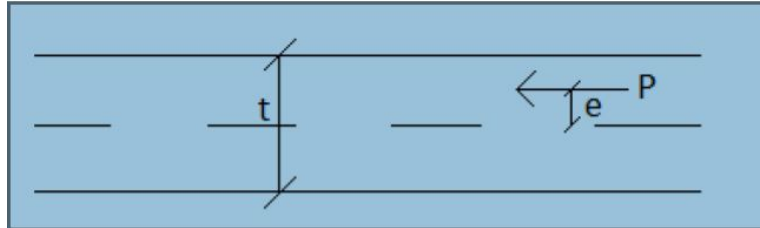


Figure 59: thrustline within the middle 1/3

When this occurs it also means that there is no tension found in the arch.

### 3.3.5 Load combinations and factors

To obtain sufficient safety for this design it is necessary to adhere to the Eurocodes in terms of standards and load combinations on the pavilion. There are two separate limit states that can be reached with the pavilion, those being serviceability and ultimate limit states. The former meaning that there will be the need for maintenance and the latter that the state of the pavilion will be that of a collapsed structure beyond repair. These equations can be expressed as:

#### U.L.S

$$\sum_{j \geq 1} \gamma_{Gj} G_{kj} + \gamma_P P_k + \gamma_{Q1} Q_{k1} + \sum_{i > 1} \gamma_{Qi} \psi_{0i} Q_{ki}$$

#### S.L.S

Characteristic combination

$$\sum_{j \geq 1} G_{kj} + P_k + Q_{k1} + \sum_{i > 1} \psi_{0i} Q_{ki}$$

Action	$\psi_0$	$\psi_1$	$\psi_2$
Imposed loads in buildings, category (see EN 1991-1-1)			
Category A : domestic, residential areas	0,7	0,5	0,3
Category B : office areas	0,7	0,5	0,3
Category C : congregation areas	0,7	0,7	0,6
Category D : shopping areas	0,7	0,7	0,6
Category E : storage areas	1,0	0,9	0,8
Category F : traffic area, vehicle weight $\leq 30\text{kN}$	0,7	0,7	0,6
Category G : traffic area, $30\text{kN} < \text{vehicle weight} \leq 160\text{kN}$	0,7	0,5	0,3
Category H : roofs	0	0	0
Snow loads on buildings (see EN 1991-1-3)*			
Finland, Iceland, Norway, Sweden	0,70	0,50	0,20
Remainder of CEN Member States, for sites located at altitude $H > 1000\text{ m a.s.l.}$	0,70	0,50	0,20
Remainder of CEN Member States, for sites located at altitude $H \leq 1000\text{ m a.s.l.}$	0,50	0,20	0
Wind loads on buildings (see EN 1991-1-4)	0,6	0,2	0
Temperature (non-fire) in buildings (see EN 1991-1-5)	0,6	0,5	0

NOTE The  $\psi$  values may be set by the National annex.  
\* For countries not mentioned below, see relevant local conditions.

Figure 60: Safety factors for the different types of loads

Load Case	Self-weight	Wind Load	Undistributed Snow load	Redistributed Snow Load
LC1(SLS)	1	1		
LC2(SLS)	1		1	
LC3(SLS)	1			1
LC4(ULS)	1.35	1.5		
LC5(ULS)	1.35		1.5	
LC6(ULS)	1.35			1.5

Table 5: Load combinations used

#### SLS

$$\text{Load case 1 - } 1G + 1(\text{Wind load}) = 1(2.4) + 1(0.4459) = 2.8459 \text{ KN/m}^2$$

$$\text{Load case 2 - } 1G + 1(\text{Undistributed snow load}) = 1(2.4) + 1(0.56) = 2.96 \text{ KN/m}^2$$

$$\text{Load case 3 - } 1G + 1(\text{Redistributed snow load}) = 1(2.4) + 1(0.55) = 2.95 \text{ KN/m}^2$$

#### ULS

$$\text{Load case 4 - } 1.35G + 1.5(\text{Wind load}) = 1.35(2.4) + 1.5(0.4459) = 3.91 \text{ KN/m}^2$$

$$\text{Load case 5 - } 1.35G + 1.5(\text{Undistributed snow load}) = 1.35(2.4) + 1.5(0.56) = 4.08 \text{ KN/m}^2$$

$$\text{Load case 6 - } 1.35G + 1.5(\text{Redistributed snow load}) = 1.35(2.4) + 1.5(0.55) = 4.065 \text{ KN/m}^2$$

## 4. Results

### 4.1 Results and discussion of MCA

In the table below, the comparative analysis of five textiles is presented, based on the seven criteria already discussed in chapter 3.

	Tensile strength (5%)	Cost of material (30%)	Workability (5%)	CO2 footprint (30%)	Density / self weight (10%)	Energy consumption (15%)	Compatibility (5%)	Results
ampliTex	0/10	10/10	0/10	10/10	6/10	8/10	6/10	8.1
powerRibs	2/10	8/10	6/10	10/10	8/10	8/10	0/10	7.8
Jute	3/10	8/10	8/10	10/10	10/10	10/10	10/10	8.95
Carbon Fibre	10/10	0/10	0/10	0/10	5/10	0/10	10/10	1.5
AR glass fibres	7/10	4/10	10/10	6/10	0/10	6/10	7/10	5.1

Table 6: Multi Criteria Analysis

The assigned points were deduced from the literature review conducted in chapter 2. For all the criteria the scoring was made between 0 and 10, where 0 is the worst scoring textile and 10 is the textile with the highest potential. The remainder of the scores are allocated based upon a proportional linear relationship.

These scores were then used to calculate the final result by using the weightings of each of the criteria as a multiplier for each of their individual scores and then adding all the results to get a final score out of 10.

It can then be seen that the textile with the highest score was Jute as it scored the highest in 4 of the criteria, mainly focused on its environmental impact.

Unfortunately it was not possible to test the applicability of Jute textiles, due to the closing of the lab during these times of lockdown and quarantine. Therefore, the design of the pavilion is carried out with the use of carbon fibre, which is the textile with more available literature data.

## 4.2 Results and discussion of lab testing<sup>1</sup>

In this research a ratio was decided on to remain consistent throughout the tests. This ratio can be found below.

Cement CEM I 52.5 R(c)	22.2%
Fly ash	7.9%
Silica fume	1.6%
Water	12.7%
Superplasticizer	0.5%
Anker fill	22.7%
Siliceous sand	32.4%

Table 7: Mixture ratios

### 4.2.1 Consistency test

The result of the consistency test was a measurement of 60 mm slump of the mixture once the Abrams cone was lifted and placed next to the concrete pile.



Figure 61: Slump Test Results

From this result in reference to figure 62 below it can be determined that the workability of the concrete is of the class S2. This means that it is semi plastic in workability, making it able to penetrate the fibers of

---

<sup>1</sup> Disclaimer: some of the tests presented in the methodology chapter could not be carried out due to the closure of the laboratory facilities, which followed the outbreak of the Covid19. This chapter will present only the results of the tests that were actually carried out.

the textiles whilst still having enough high enough viscosity to be able to create curved precast elements without flowing to the bottom before setting.

► Consistentieklassen (op te geven door aannemer)			
Aanduiding	Verdichtingsmaat c	Zetmaat (mm) h	Schudmaat (mm)
Droog	C0	≥1,46	
Aardvochtig	C1	1,45–1,26	S1 (30–40) F1 (≤340)
Halfplastisch	C2	(1,25–1,11)	S2 50–90 F2 (350–410)
Plastisch	C3	(1,10–1,04)	S3 100–150 F3 (420–480)
Zeer plastisch		S4 (160–210)	F4 490–550
Vloeibaar		S5 (≥220)	F5 560–620
Zeer vloeibaar			F6** (≥630)

Verdichtingsmaat c =  $\left(\frac{h_0}{h_1}\right) \cdot 100$

Zetmaat (mm)

Schudmaat (mm)

\* Voor schudmaat aangepaste kegels H=200 mm gebruiken (1x x schudden).  
 \*\* Voor zelfverdichtend beton vloeimaat en stabiliteit volgens BRL 1801 en CUIF-aanbeveling 93.

Figure 62: Slump Test Classification Table

#### 4.2.2 Air content test

After the steps were followed according to the procedure it was found that the air content of the concrete was 4% as can be seen in figure 63 below. The air content is important in concrete as it works as a buffer when it comes to freezing and thawing cycles. This is because it relieves some of the pressure caused by the expansion of water when it freezes. These air bubbles also reduce the strength of the concrete and therefore need to be kept to a low percentage.



Figure 63: Air Content of Concrete

#### 4.2.3 Density

The concrete cubes had been cured for 7 days; these cubes were then measured and weighed to determine the density of the concrete mixture once it had hardened.

Three cubes were measured and their dimensions, weights and densities were as follows:

	Dimensions (mm)	Weight (g)	Density (kg/m <sup>3</sup> )
FG-1	150*150*150	7196	2132.148
FG-2	150*150*149	7148	2132.14
FG-3	150*150*149	7155	2134.2

Table 8: Dimensions, weights and densities of the cubes

#### 4.2.4 Compressive test

In table 8 below presents the results of the compressive tests for the three concrete cubes aged 7 days. From these cubes an average compressive strength of 50.35 N/mm<sup>2</sup> was found at 7 days of curing.

Date of testing	Cube code	Dimensions (mm)	Load (kN)	Strength (N/mm <sup>2</sup> )		Average strength (N/mm <sup>2</sup> )
				7 days	28 days	
12/03/2020	FG-1	150*150*150	871.2	38.71	-	50.35
12/03/2020	FG-2	150*150*149	1263.6	56.16	-	
12/03/2020	FG-3	150*150*149	1278.1	56.8	-	
	FG-4			-		
	FG-5			-		
	FG-6			-		

Table 9: Results from the compressive tests done on cubes

When this result is compared with figure 64 below it can be seen that a concrete compressive strength of 50.35 N/mm<sup>2</sup> is higher than what would commonly be expected of concrete with CEM I 52.5 R(c) which would be 34.13 N/mm<sup>2</sup>.

### Compressive Strength of Concrete at Various Ages

The strength of concrete increases with age. The table shows the strength of concrete at different ages in comparison with the strength at 28 days after casting.

Age	Strength percent
1 day	16%
3 days	40%
7 days	65%
14 days	90%
28 days	99%

Figure 64: Concrete compressive strength ratios (Mishra, G., 2020)

### 4.3 Results and discussion of pavilion design

Once the ULS forces were found they were implemented in the Matlab model to find the stress, strain and displacement of the pavilion. From ULS forces the largest was chosen as it would be considered the worst case scenario. This force was found to be a distributed load of  $4.08 \text{ KN}/\text{m}^2$ . The following results were produced. The pavilion was modelled as a 1 meter width basis for ease of construction and implementation during installation and transport. These sections will then be connected on site as seen in the technical drawings.

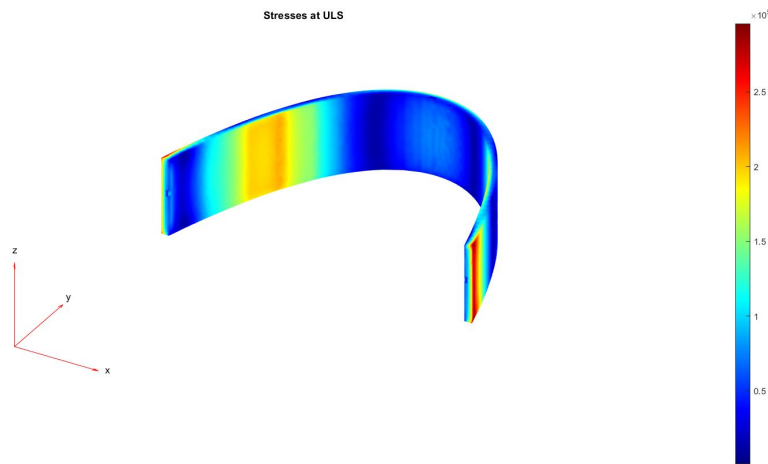


Figure 64: Stresses found in pavilion

When the ULS forces were applied to the pavilion in matlab the stress distribution as seen in figure 64 above was highly varied with a maximum stress of  $3 \cdot 10^5 \text{ N}/\text{m}^2$ . These stresses were found at the bases of the pavilion, as can be seen from the red colouration in those areas; this result is consistent with the expectations, since all the stresses are transferred along the pavilion towards the supports, and thus that is where the forces accumulate.

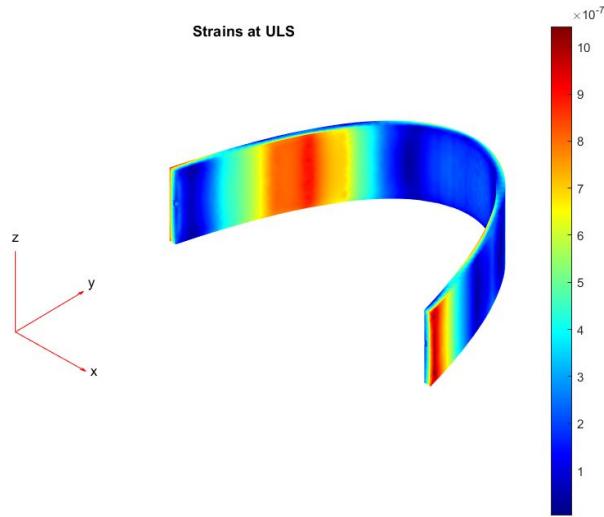


Figure 65: Strains found in the pavilion at ULS

The maximum strains found in the pavilion were found at four separate locations as seen in figure 65 above labelled in red. Those being the two bases on the external surfaces and half way up on either side on the internal surfaces. The maximum strain reached was found to be  $10.5 \cdot 10^{-7}$ . These strains are mainly related to the wind load on the pavilion which shifts the pavilion in a horizontal direction causing strains in those areas. This is consistent with the typical locations for the formation of hinges in an arch, caused by the shifting of the thrust line, as presented in figure 21.

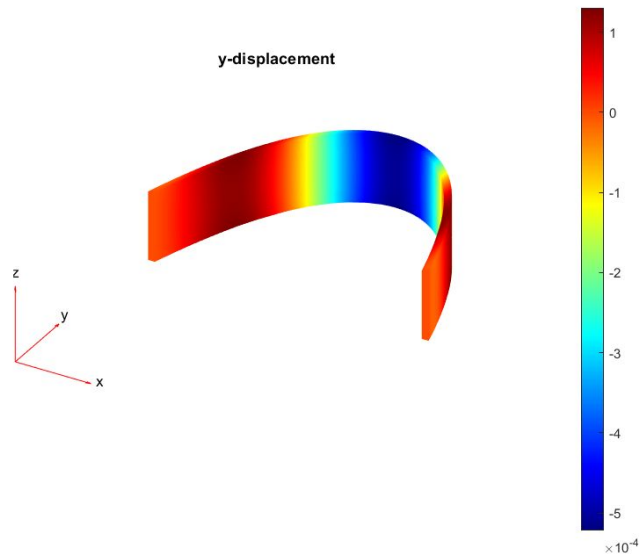


Figure 66: Vertical displacement at ULS

Figure 66 above displays the vertical displacement that will occur in the pavilion when the ULS load is applied to it. This is related to the self weight of the pavilion, the snow load as well as the wind load of

the top of the pavilion as they are all acting in a vertical direction, specifically downward. From the figure it can be seen by the (dark blue colour) at the top of the pavilion which represents the largest displacement of  $5.1 \cdot 10^{-4}mm$ .

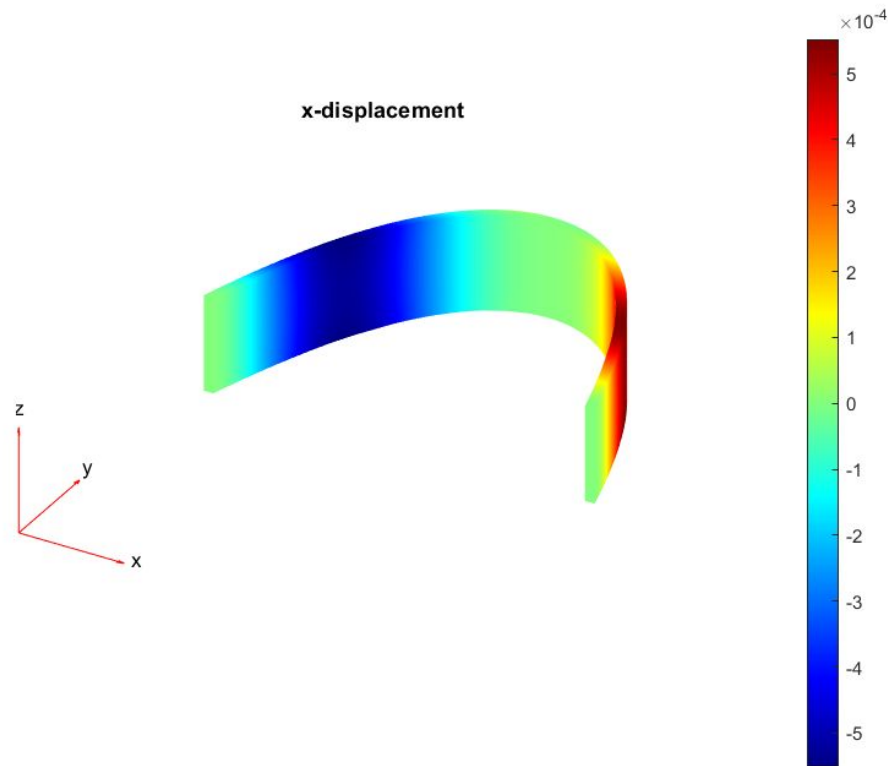


Figure 67: Horizontal displacement at ULS

Figure 67 above displays the horizontal displacement that will occur in the pavilion when the ULS load is applied to it. This displacement is due to the horizontal wind loads applying pressure on the surfaces of the pavilion. From the model above it can be seen that the maximum horizontal displacement was  $5.3 \cdot 10^{-4}mm$ .

The results from these models were then used in the calculations below to verify the safety of the pavilion in terms of buckling, cracking and stability.

#### 4.3.1 Buckling checks

This gives the equation:

$$q_{cr} = \gamma_4 \cdot \frac{EI}{R^3}$$

$$q_{cr} = 96.24 \cdot \frac{0.25 \cdot 10^5 \cdot 8.33 \cdot 10^{-5}}{2^3}$$

$$q_{cr} = 25.05 \text{ KN/m}^2$$

As can be seen this value is higher than that found from the ULS combination and thus the Pavilion is safe from a buckling load.

$$P_{crit} = \frac{2}{\sqrt{3(1-\nu^2)}} \cdot E \left( \frac{t}{a} \right)$$

$$P_{crit} = \frac{2}{\sqrt{3(1-0.15^2)}} \cdot 0.25 \cdot 10^5 \cdot \left( \frac{0.1}{2} \right)$$

$$P_{crit} = 1459.893 \frac{KN}{m^2}$$

This gives us a critical load of 1459.893 kN/m<sup>2</sup>.

It is possible to calculate the self-weight per meter of the arch by taking the self-weight of concrete which is 25 kN/m<sup>2</sup> and multiplying it by the volume of one half of the archway. Thus giving a total self-weight of 18.13kN/m<sup>2</sup>.

That means that the structure could withstand a load 8.05 times its own weight. In order to get a safer idea of the real life strength of the pavilion it is necessary to apply the knockdown factor (Hutchinson, J. W. 2010). This factor is used as a reduction factor to account for the imperfections that could be found in the structure once it is actually built. With the use of this knockdown factor of 1/8 the pavilion can withstand a load equal to 1.34 times its self weight.

#### 4.3.2 Crack control

$$\varepsilon = \frac{\omega}{h} \Rightarrow \omega = \varepsilon * h = 10.5 \cdot 10^{-7} \cdot 7253 = 7.616 \cdot 10^{-3} mm$$

From the equation above it can be seen that the maximum strain found in the pavilion at ULS gives a crack width of  $7.617 \cdot 10^{-3} mm$ . This value is lower than the recommendations provided by AFGC state the following values for crack widths which are:

- 0.3 mm for highly detrimental cracking
- 0.2 mm for detrimental cracking
- 0.1 mm for normal cracking

This proves that the pavilion will not fail due to cracking.

#### 4.3.4 Stability check

The shift of the thrustline due to displacement in relation to the thickness of the arch is:

$$5.5 \cdot 10^{-4} < \frac{1}{6} t$$

$$5.5 \cdot 10^{-4} < 1.67 mm$$

Therefore according to the safe theorem developed by Heymans (1966) the pavilion will not develop any hinges and will therefore be stable under the ULS loads applied to it.

## 5. Discussion and Conclusions

The goal of this research was to set up suitable laboratory tests and analysis methods for the strength and durability testing of bio-based textile reinforced concrete. This thesis was a preparatory research for the actual development of bio-based TRC applications, which was not undertaken due to unforeseen limitations. These were caused by the closing of the labs due to quarantine for the COVID-19 virus. With Textile Reinforced Concrete being a composite material with a heterogeneous structure, it was important to evaluate the properties of the individual materials and their composite action to gain an understanding of the composite behaviour of a structure made from it. This was done through the form of literature review and an MCA. These two forms of evaluation gave the final result that the best textile reinforcement from the chosen textiles that were researched was the Jute textile. This was due to its low environmental impact when compared to the more commonly used textiles such as carbon fibre and AR glass fibres (van Dam, 2008), as well as its high strength when being compared to its fellow biobased textiles such as ampliTex and powerRibs (Sett et al. 2000). The Jute textile scored the highest score of 10 out of 10 in 4 out of 7 of the different criteria assessed in the MCA, these being CO2 footprint, Density, Energy consumption and Compatibility. The criteria where it did not score the highest were Tensile strength, where it scored the highest of the biobased textiles, Cost of material where it was second highest with 8 out of 10 and Workability where it also came second with 8 out of ten. This shows that the textile itself was dominant throughout all criteria in the MCA.

Summarizing, throughout the process of researching the biobased textile reinforcements the different aspects of the reinforcement, both biobased and more commonly used as a comparison, were found and analysed, namely, their benefits, limitations and costs. These were then used to decide whether the use of biobased textiles were beneficial to the construction. Although they were found to be beneficial, one of the negative factors found for when dealing with biobased textiles was the need for pretreatments of the textile to ensure cohesion and compatibility between it and the concrete matrix. This aspect was not investigated in this research context due to limited access to the laboratory facilities, but it definitely requires further research and analysis in the future.

The work in the lab took place at the beginning of the research and was cut short as previously mentioned. The cubes that were tested for the 7 days strength performed well with a compressive strength of  $50.35 \text{ N/mm}^2$  and with an indication of common concrete strength with CEM I 52.5 R(c) being  $34.13 \text{ N/mm}^2$  (Mishra, G., 2020). Further testing is required for the 28 day tests to see whether it follows the common concrete final strength or whether it surpasses it.

This thesis presents also a possible application for this new technology, by developing the design of a thin shell textile reinforced concrete shell structure pavilion. In this phase, the pavilion was verified by imagining a carbon fiber reinforcement, keeping in mind that in the future, the application using biobased textiles must be investigated by using laboratory testing on scaled models. The design was done through multiple stages. Starting with the research of arches and their stability which revealed the safe theorem by Heymans (1966), which discusses the line of thrust of an arch and how it affects the stability of the arch. This principle was then used as the main factor when designing the pavilion, this led to the use of a catenary curve for the design of the pavilion as it is designed to follow the line of thrust and thus increasing the stability but also reducing the tensile forces in the arch under its own self weight to 0. The

catenary curve is the best option to implement biobased textiles due to the reduced tension in the structure. Courtesy of the shape of the curve all of the forces are felt in compression and therefore it is possible to use a textile reinforcement with a lower tensile strength which is the main area in which the biobased textiles underperformed in relation to the more commonly used textiles.

This design is a common shape used in sustainable housing in South Africa as seen in Surat (2017), Le Roux (2017) and Bulovic (2014). This was found to be more effective than expected as when the model was tested with the application of the ULS loads it was found that even under the effects of external forces including wind and snow load that there were no tensile forces found in the arch, but rather the whole arch experienced compressive forces. In this model that was made in AutoCAD and tested in MatLab it was seen that the highest strains found in the the bases of the pavilion as well as the points at which the angle of the catenary curve became more horizontal than vertical , this correlates with Figure 21 found in chapter 2.4 which show an arch that has developed hinges due to instability. Thus the maximum strains will also be found in these regions. The stresses, strains and displacements found in the MatLab model were then used in the buckling check, critical load, crack control and stability checks. All of these checks were passed by the pavilion with a lot of room for optimisation, with the exception of the critical load which was found to be only 1.34 times the self weight of the pavilion. This may restrict future optimisations.

Based on the points discussed above it can be concluded that the project was able to set up suitable laboratory tests and analysis methods for the strength and durability of biobased textile reinforced concrete, and thus complete all the objectives of the project and answer all the research questions. Additionally, the methods deemed necessary by the regulations and requirements for the design of the textile reinforced concrete shell structure were implemented and the results found validated that the design was viable.

## 6. Recommendations

Based on the research results produced during this thesis, the design of a catenary pavilion made of TRC is ultimately advised as feasible. The design allows lower material use than usual concrete technologies, thanks to the limited concrete cover required. This finally results in a very light structure, easy and inexpensive to transport and to use. Therefore, the pavilion appears as a good solution for temporary exposition spaces.

The following recommendations are developed to further optimize the design of the pavilion:

- An attempt could be made to optimise the design of the pavilion. This could be done in terms of thickness of the arch, as it was seen that in the majority of the tests the design surpassed the actual loads. Therefore further research into why the critical load was lower in relation to the other checks.
- The use of additional analysis softwares such as eTabs, SAP2000 or STAAD Pro is recommended to verify the results found in the MatLab model.
- The connection plates between the panels need to be accurately calculated based on parameters like bond strength and tensile stresses developing within the shell. These calculations may additionally slightly modify the form and/or orientation on panels.
- A design of the foundation of the pavilion can be made so that it can be properly constructed to a realistic scale. A recommendation for the style of foundation would be a bucket foundation as it doesn't affect the original design of the pavilion but rather acts as a slot in which the pavilion can be inserted.
- Further tests are necessary to allow the conversion of the pavilion to biobased TRC. These tests include pretreatment analysis, mechanical tests and durability tests. On the other hand, the design appears suitable for the application of this new technology, thanks to the very limited tensile stresses present in the structure.
- Further laboratory research with physical scale models are advised to verify the dynamic behaviour of the pavilion and to compare it with the MATLAB results.

## 7. Bibliography

ACI Education Bulletin E2-00. (2000): ACI Education Bulletin E2-00: Reinforcement for Concrete - Materials and Applications (Reapproved 2006). ACI Committee E-701, American Concrete Institute.

Asokan, P., Firdoous, M., & Sonal, W. (2012). Properties and potential of bio fibres, bio binders, and bio composites. *Rev. Adv. Mater. Sci*, 30(3), 254-261.

Benhelal, E., Zahedi, G., Shamsaei, E., & Bahadori, A. (2013). Global strategies and potentials to curb CO<sub>2</sub> emissions in cement industry. *Journal of cleaner production*, 51, 142-161.

Bentur A. and Mindess S. (2006): Fibre reinforced cementitious composites. CRC Press.

Bentland, S. (2015). Towards Ultra-thin Façade Elements-Textile Reinforced Green Concrete with Vacuum Insulation Panels (Master's thesis).

Block, P., DeJong, M., & Ochsendorf, J. (2006). As hangs the flexible line: Equilibrium of masonry arches. *Nexus Network Journal*, 8(2), 13-24.

Bramshuber W. (ed.) 2006. Report 36: Textile Reinforced Concrete-State-of-the-Art Report of RILEM TC 201-TRC: RILEM publications.

Bulovic, I., 2014. Catenary vaults: a solution to low-cost housing in South Africa. Johannesburg. MSc. University of Witwatersrand.

Butler M., Mechtcherine V. and Hempel S. (2009): Experimental investigations on the durability of fibre–matrix interfaces in textile-reinforced concrete. *Cement and Concrete Composites*, Vol. 31 (4), pp. 221-231.

Büttner, T., Alessandra, K., & Raupach, M. (2008, April). Improvement of load-bearing capacity and durability of textile-reinforced concrete due to the use of polymers. In 15th Congress of the Glassfibre Reinforced Concrete Association International, Prague, Czech Republic (pp. 20-23).

Büttner T., et al. (2010): Enhancement of the Durability of Alkali-resistant Glass- Rovings in concrete. International RILEM Conference on Material Science, Germany, 2010: RILEM Publications SARL, pp. 333-342.

Cauberg, N., Tysmans, T., Adriaenssens, S., Wastiels, J., Mollaert, M., & Belkassam, B. (2012). Shell elements of textile reinforced concrete using fabric formwork: a case study. *Advances in Structural Engineering*, 15(4), 677-689.

Cruz, C. M., Gohil, U., Quadflieg, T., Raupach, M., & Gries, T. IMPROVING THE BOND BEHAVIOR OF TEXTILE REINFORCE-MENT AND MORTAR THROUGH SURFACE MODIFICATION.

Cherkas, A., & Rimshin, V. (2017). Application of composite reinforcement for modernization of buildings and structures. In MATEC Web of Conferences (Vol. 117, p. 00027). EDP Sciences.

Chudoba, Rostislav & Sharei, Ehsan & Scholzen, A.. (2016). A strain-hardening microplane damage model for thin-walled textile-reinforced concrete shells, calibration procedure, and experimental validation. *Composite Structures*. 152. 913–928. 10.1016/j.compstruct.2016.06.030.

Curbach M. and Jesse F. (1999): High-Performance Textile-Reinforced Concrete. *Structural Engineering International*, Vol. 9 (4), pp. 289-291.

Davidovits, J. (1994). Global warming impact on the cement and aggregates industries. *World resource review*, 6(2), 263-278.

Dejke V. (2001): Durability of FRP reinforcement in concrete: literature review and experiments. Licentiate Thesis, Building Materials, Chalmers University of Technology.

De Bolster, E., Cuypers, H., Van Itterbeeck, P., Wastiels, J., & De Wilde, W. P. (2009). Use of hyper-shell structures with textile reinforced cement matrix composites in lightweight constructions. *Composites Science and Technology*, 69(9), 1341-1347.

Engberts, E. (2006). Large-size facade Elements of textile reinforced concrete. In ICTRC'2006-1st International RILEM Conference on Textile Reinforced Concrete (pp. 309-318). RILEM Publications SARL.

Fanguero R. (2011): Fibrous and composite materials for civil engineering applications. Elsevier.

Fujisaki T., Nakatsuji T. and Sugita M. (1993): Research and development of grid shaped FRP reinforcement. *ACI Special Publication*, Vol. 138.

Fu, S. Y., Lauke, B., Mäder, E., Yue, C. Y., & Hu, X. (2000). Tensile properties of short-glass-fiber-and short-carbon-fiber-reinforced polypropylene composites. *Composites Part A: Applied Science and Manufacturing*, 31(10), 1117-1125.

Gill, A., Vitsotsky, D., Mears, L., Summers, J.(2016). Cost Estimation Model for PAN Based Carbon Fiber Manufacturing Process

Häubler-Combe, U., & Hartig, J. (2007). Bond and failure mechanisms of textile reinforced concrete (TRC) under uniaxial tensile loading. *Cement and concrete composites*, 29(4), 279-289.

Hall, T., & Ghali, A. (2000). Long-term deflection prediction of concrete members reinforced with glass fibre reinforced polymer bars. *Canadian Journal of Civil Engineering*, 27(5), 890-898.

Harris, C.M., 2006. Dictionary of architecture & construction, McGraw-Hill

Hayashi R., et al. (1990): Tensile Properties of Carbon Fiber Mesh Reinforced Mortar with Various Weavings. *Proceedings of the Japan Concrete Institute*, 1990, pp. 1043-1048.

Hegger, J., Will, N., Bruckermann, O., & Voss, S. (2006). Load-bearing behaviour and simulation of textile reinforced concrete. *Materials and structures*, 39(8), 765-776.

- Hegger, J., Zell, M., & Horstmann, M. (2008, May). Textile reinforced concrete—realization in applications. In Proceedings: international fib symposium tailor made concrete structures: new solutions for our society (pp. 357-362).
- Hegger J., et al. (2010): Sandwich Panels Made of TRC and Discrete and Continuous Connectors. International RILEM Conference on Material Science - 2nd ICTRC - Textile Reinforced Concrete - Theme 1, Brameshuber, W. (ed.) Aachen 2010a: RILEM Publications SARL, pp. 381-392.
- Hewlett, P., & Liska, M. (Eds.). (2019). *Lea's chemistry of cement and concrete*. Butterworth-Heinemann.
- Heyman, J., 1966. The stone skeleton. *International Journal of Solids and Structures*, 2(2), pp.249–279
- Huerta, S. (2005). The use of simple models in the teaching of the essentials of masonry arch behaviour. *Theory and Practice of Construction: Knowledge, Means, and Models*, Ravenna: Ed. G. Mochi, 747-761.
- Hutchinson, J. W. (2010). Knockdown factors for buckling of cylindrical and spherical shells subject to reduced biaxial membrane stress. *International Journal of Solids and Structures*, 47(10), 1443-1448.
- Ineson, P. R. (1990). Siliceous components in aggregates. *Cement and Concrete Composites*, 12(3), 185-190.
- Karus, M., & Kaup, M. (2002). Natural fibres in the European automotive industry. *Journal of Industrial Hemp*, 7(1), 119-131.
- Katz A. and Bentur A. (1996): Mechanisms and processes leading to changes in time in the properties of CFRC. *Advanced Cement Based Materials*, Vol. 3 (1), pp. 1-13.
- Kochova, K.; et al., 2016. Use of alternative organic fibres in cement composites. , pp.1–8.
- Kutschera, M., Breiner, T., Wiese, H., Leitl, M., & Braeu, M. (2009). Nano-modification of building materials for sustainable construction. In *Nanotechnology in Construction 3* (pp. 275-280). Springer, Berlin, Heidelberg.
- Le, H. T., Müller, M., Siewert, K., & Ludwig, H. M. (2015). The mix design for self-compacting high performance concrete containing various mineral admixtures. *Materials & Design*, 72, 51-62.
- Le Roux, J. S. (2017). *The optimisation and design of catenary barrel vaults for excessive wind load* (Doctoral dissertation).
- Machida A. and Gakkai D. (1993): State-of-the-art report on continuous fiber reinforcing materials. Research Committee on Continuous Fiber Reinforcing Materials, Japan Society of Civil Engineers.
- Mahadevan M. G. (2009): *Textile Spinning, Weaving and Designing*. Chandigarh, IND, Global Media.
- Majumdar, A. J., West, J. M., & Larnar, L. J. (1977). Properties of glass fibres in cement environment. *Journal of Materials Science*, 12(5), 927-936.
- Mathijssen, D. (2018). The renaissance of flax fibers. *Reinforced Plastics*, 62(3), 138-147.

- Mazloom, M., Ramezaniapour, A. A., & Brooks, J. J. (2004). Effect of silica fume on mechanical properties of high-strength concrete. *Cement and Concrete Composites*, 26(4), 347-357.
- Mehta, P. K. (2002). Greening of the concrete industry for sustainable development. *Concrete international*, 24(7), 23-28.
- Mehta P. K., Monteiro P. J. and Education M.-H. (2006): *Concrete: microstructure, properties, and materials*. McGraw-Hill New York.
- Micelli F. and Nanni A. (2004): Durability of FRP rods for concrete structures. *Construction and Building Materials*, Vol. 18 (7), pp. 491-503.
- Mishra, G. (2020, April 17). Compressive Strength of Concrete -Cube Test, Procedure, Results. Retrieved May 29, 2020, from <https://theconstructor.org/concrete/compressive-strength-concrete-cube-test/1561/>
- Möller, B., Graf, W., Hoffmann, A., & Steinigen, F. (2005). Numerical simulation of RC structures with textile reinforcement. *Computers & structures*, 83(19-20), 1659-1688.
- Nawy, E. (2000). *Reinforced concrete: A fundamental approach*.
- Newcomb, B. A., & Chae, H. G. (2018). The properties of carbon fibers. In *Handbook of Properties of Textile and Technical Fibres* (pp. 841-871). Woodhead Publishing.
- Ohno S. and Hannant D. (1994): Modeling the Stress-Strain Response of Continuous Fiber Reinforced Cement Composites. *ACI Materials Journal*, Vol. 91 (3).
- Orlowsky J., et al. (2005): Durability modelling of glass fibre reinforcement in cementitious environment. *Materials and Structures*, Vol. 38 (2), pp. 155-162.
- Papanicolaou, C. G., & Papantoniou, I. C. (2010). Mechanical behavior of textile reinforced concrete (TRC)/concrete composite elements. *Journal of Advanced Concrete Technology*, 8(1), 35-47.
- Peerdeman, B. (2008). Analysis of thin concrete shells revisited: Opportunities due to innovations in materials and analysis methods. Master's thesis the Netherlands: Delft University of Technology, 30-50.
- Purnell P. (1998): The durability of glass fibre reinforced cements made with new cementitious matrices. Dissertation, Aston University
- RILEM Technical Committee 232-TDT (Wolfgang Brameshuber) brameshuber@ibac.rwth-aachen.de. (2016). Recommendation of RILEM TC 232-TDT: test methods and design of textile reinforced concrete: Uniaxial tensile test: test method to determine the load bearing behavior of tensile specimens made of textile reinforced concrete. *Materials and Structures*, 49, 4923-4927.
- Scheerer S., Schladitz F. and Curbach M. (2015): *Textile Reinforced Concrete - From the Idea to a High Performance Material*. 3rd ICTR International Conference on Textile Reinforced Concrete Brameshuber, W. (ed.) Aachen, Germany, 2015: RILEM SARL, pp. 15-33.

Scheffler C., et al. (2009): Interphase modification of alkali-resistant glass fibres and carbon fibres for textile reinforced concrete I: Fibre properties and durability. *Composites Science and Technology*, Vol. 69 (3), pp. 531-538.

Scheffler C., et al. (2009): Interphase modification of alkali-resistant glass fibres and carbon fibres for textile reinforced concrete I: Fibre properties and durability. *Composites Science and Technology*, Vol. 69 (3), pp. 531-538.

Scheffler, C., Gao, S. L., Plonka, R., Mäder, E., Hempel, S., Butler, M., & Mechtcherine, V. (2009). Interphase modification of alkali-resistant glass fibres and carbon fibres for textile reinforced concrete II: Water adsorption and composite interphases. *Composites Science and Technology*, 69(7-8), 905-912.

Schneider, H. N. et al. 2006. Textile Reinforced Concrete – Applications and Prototypes. Proceedings of the 1st international RILEM Symposium on Textile Reinforced Concrete (ICTRC), Aachen, 2006, S. 297–307.

Sett, S. K., Mukherjee, A., & Sur, D. (2000). Tensile characteristics of rotor and friction spun jute blended yarns. *Textile research journal*, 70(8), 723-728.

Shakor, P. N., & Pimplikar, S. S. (2011). Glass fibre reinforced concrete use in construction. *International Journal of Technology and Engineering System*, 2(2), 632-634.

Sharrard, A. L., Matthews, H. S., & Ries, R. J. (2008). Estimating construction project environmental effects using an input-output-based hybrid life-cycle assessment model. *Journal of Infrastructure Systems*, 14(4), 327-336.

Sim J., Park C. and Moon D. Y. (2005): Characteristics of basalt fiber as a strengthening material for concrete structures. *Composites Part B:Engineering*, Vol. 36 (6–7), pp. 504-512.

Surat, D. (2017). Seismic analysis of thin shell catenary vaults (Doctoral dissertation).

Thomas, N.L. & Birchall, J.D., 1983. The retardation action of sugars on cement hydration. *CEMENT and CONCRETE RESEARCH*, 13, p.12.

van Dam, J. E. (2008). Natural fibres and the environment: environmental benefits of natural fibre production and use. In Proceedings of the Symposium on Natural Fibres: Common fund for commodities, 20 October 2008, Rome, Italy, (pp. 3-17).

Wesche, K. (Ed.). (1991). Fly ash in concrete: properties and performance. CRC Press.

Wiik, M. R. K., Thorhallsson, E. R., & Azrague, K. (2017). A mechanical and environmental assessment and comparison of basalt fibre reinforced polymer (BFRP) rebar and steel rebar in concrete beams.

Williams Portal, N. (2015). Usability of Textile Reinforced Concrete: Structural Performance, Durability and Sustainability. Chalmers University of Technology.

Wulfhorst B., et al. (2006): Textile technology. Wiley Online Library.

“AmpliTex™.” Natural Fibre Fabrics, [www.bcomp.ch/en/products/amplitex](http://www.bcomp.ch/en/products/amplitex).

# Appendices

## Appendix 1

		Name	Duration	Start	Finish
1		Start of thesis	1 day?	2020/01/31 ...	2020/01/31...
2		Start document	11 days	2020/01/31 ...	2020/02/14...
3		Research proposal	34 days?	2020/02/14 ...	2020/04/01...
4		Lab tests(make the cubes)	1 day?	2020/02/17 ...	2020/02/17...
5		Lab test(make the mould f...	1 day?	2020/02/18 ...	2020/02/18...
6		Lab test(make the slabs)	4 days?	2020/02/20 ...	2020/02/25...
7		Lab tests(test the cubes)	1 day?	2020/03/17 ...	2020/03/17...
8		In school presentations	1 day?	2020/04/01 ...	2020/04/01...
9		In company meeting	1 day?	2020/04/07 ...	2020/04/07...
10		Finish structural checks list	15 days?	2020/04/07 ...	2020/04/27...
11		Work on schedule of requi...	1 day?	2020/04/28 ...	2020/04/28...
12		Finish methodology	3 days?	2020/04/29 ...	2020/05/01...
13		Finish research on shell str...	1 day?	2020/05/02 ...	2020/05/04...
14		Use matlab to analyse pav...	11 days?	2020/05/02 ...	2020/05/18...
15		Do the structural checks f...	3 days?	2020/05/19 ...	2020/05/21...
16		Finish boundary conditions	1 day?	2020/05/23 ...	2020/05/25...
17		Conclusions and recomme...	1 day?	2020/05/24 ...	2020/05/25...
18		Finish drawings	1 day?	2020/05/25 ...	2020/05/25...
19		Hand in first draft	1 day?	2020/05/25 ...	2020/05/25...
20		Fix report based on feedb...	9 days?	2020/05/26 ...	2020/06/05...
21		Submit thesis	1 day?	2020/06/05 ...	2020/06/05...
22		Thesis defence	1 day?	2020/06/24 ...	2020/06/24...

## Appendix 2





Technical Data Sheet  
ampliTex™ Ref. 5040  
rev. a

---

**ampliTex™**  
Art. No. 5040  
twill 2/2 fabric 300 gsm



ampliTex™ 5040 is a bidirectional fabric with fibers oriented at 0° and 90°, suitable for manufacturing of high performance composite products with low environmental impact. The twill weave guarantees an ideal balance between drapability and antislip properties, suited for the manufacturing of complex parts. The use of untwisted yarns ensures high laminate stiffness.

---

**Fabric architecture**

Fibre type : Flax (EU)  
Construction : twill 2/2 weave  
Yarn Tex : 300 tex  
Fabric weight : 300 gsm +/- 5%  
150 gsm in each direction

**Dimensions**

Standard width : 1000 mm  
Standard roll length : 50 m

**Ecological Aspects**

Grown in France and Belgium, the flax used at Bcomp is a regional resource. Production of flax has a negative global warming indicator because of the CO<sub>2</sub> sequestration by photosynthesis.  
Find more details on [bcomp.ch](http://bcomp.ch).

**Technical Performances**

The flax fibres used in ampliTex™ fabrics have a modulus of about 60 GPa and a tensile strength of 800 MPa, which makes them a performing technical fibre. Comparing the specific stiffness of ampliTex™ and glass fibres shows that the tensile performance of ampliTex™ fabrics is about 50% better. Further advantages are vibration damping properties which are much greater compared to glass or carbon fibre, and less fragile fracture behavior than carbon fibre.

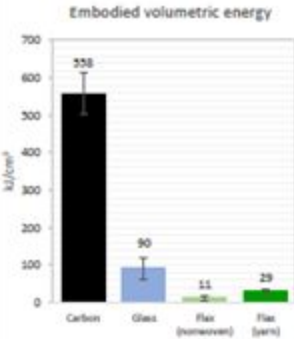
Tensile Properties	
Young's Modulus // to fibres (GPa)	19.4
Young's Modulus ⊥ to fibres (GPa)	19.4
Strength // to fibres (MPa)	149.3
Strength ⊥ to fibres (MPa)	149.3
Strain to failure // to fibres (%)	1.05
Strain to failure ⊥ to fibres (%)	1.05

Flexural Properties	
Modulus // to fibres (GPa)	17.9
Modulus ⊥ to fibres (GPa)	17.9
Strength // to fibres (MPa)	201
Strength ⊥ to fibres (MPa)	201
Yield strength, Rp0.2 // (MPa)	134

**Ply Properties**

Density dry fibers (Kg/m <sup>3</sup> )	1450
Ply thickness (mm) @ 43%   60% Vf	0.46   0.34

**Embodied volumetric energy**



Material	Embodied volumetric energy (MJ/cm <sup>3</sup> )
Carbon	538
Glass	90
Flax (nonwoven)	11
Flax (woven)	29

**Processing Guidelines**

- Excellent compatibility with epoxy and polyester
- Near-zero CTE, hence full processing compatibility with carbon fibres
- Compatible with infusion-based processes (vacuum infusion, RTM), wet layup, bladder inflation moulding (BIM) and compression moulding
- Flax fibers always contain some humidity under ambient conditions. Some resins (especially polyesters) are sensitive to moisture and may poorly polymerize or create bubbles. In this case we recommend drying the fabrics prior use (110°C for 15 minutes)
- Fibre weight fraction of 60% can be achieved with process pressure > 5 bars. However, the fibres absorb a lot of resin when hand-laminating and it tends to look "dry" (unless too much resin is used) before pressure is applied. We recommend controlling the amount of resin used for laminating and impregnating with 50 to 60% resin in weight. Excess resin will be squeezed out while pressing.

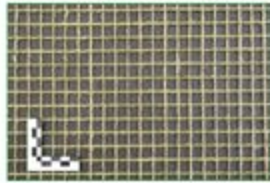
All data given is based on representative samples of the materials in question. Since the method and circumstances under which these materials are processed and tested are key to their performance, and Bcomp has no assurance of how its customers will use the material, the company cannot guarantee these properties.

Bcomp Ltd. | [www.bcomp.ch](http://www.bcomp.ch) | [contact@bcomp.ch](mailto:contact@bcomp.ch)

# Appendix 3



powerRibs  
Art. No. 5019  
0°/90°



## Product description

powerRibs, suitable for manufacturing fiber reinforced composite products with high performance and low environmental impact. This special reinforcement fabric is used to create a rib structure on one surface of the composite layer, significantly increasing the flexural stiffness and damping properties of thin composite shells with little additional weight.

### Fabric construction

Fibre type: Flax (EU)  
Construction: 0°/90°  
Fibre tex: 1500 TEX  
Fabric weight: 215 gsm +/- 5%  
Architecture: Grid-like fabric with 14 mm mesh size  
Measurements  
Standard width: 1150 mm  
Standard roll length: 50 m

### Mechanical composite properties

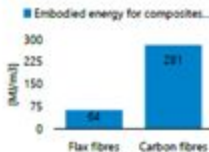
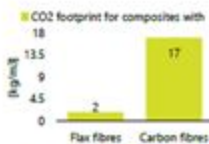
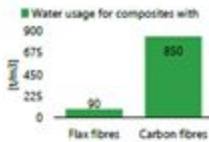
Due to the discontinuous 3D structure, the mechanical properties of the powerRibs cannot be described in a generic way. The mechanical properties of powerRibs applied to a base layer can be represented by an equivalent homogeneous layer added to the laminate. The equivalent layer represents the "smeared" effect of the powerRibs over the part's surface.  
Note that the equivalent modulus is not identical in both in-plane directions. This is due to the ribs being bonded flat to the base in one direction. However, in the other direction the ribs have to "travel" over the flat ribs at each of their intersections (see modeling FE & 3D guide for illustration).  
Due to its grid structure with big tough yarns, powerRibs provides a very high damage tolerance to the part, also ensuring that it stays in one part even when crashed.

Technical specifications	Composites*
Young's modulus in the wavy ribs direction	3.45 GPa
Young's modulus in the flat ribs direction	2.65 GPa
Shear modulus	280 MPa
Poisson's ratio	0.04
Density	363.6 kg/m <sup>3</sup>
Thickness	1.21 mm

\*These are the properties of the equivalent composite layer which can be used to simulate the effect of a powerRibs layer infused with R&G resin L and GL2 hardener, 45% Vt of fibres

### Ecological aspects

Compared to carbon fibre reinforced plastics, powerRibs composite material (flax fibre reinforced plastic) has significantly lower environmental impact due to its weight advantages and lower material input.  
Water usage, CO<sub>2</sub> footprint and embodied energy, is about 85% lower while using flax fibre reinforced plastics.



### Important facts

- PowerRibs are well compatible with epoxy, polyester or PP matrix
- Flax fibers always contain some humidity at ambient conditions. Some resins (especially polyesters) are sensitive to moisture and may badly polymerize or create bubbles. In that case, dry the fabrics before use (110°C for 15 minutes)
- The key factor to optimize the effect of the powerRibs is to create a good rib structure. Therefore a very flexible vacuum bag, or bladder has to be used, so that the bag matches as well as possible the yarns of the ribs.
- The ribs are normally used as last layer on the surface. However, it is possible to put another fabric layer on the top of it, it creates a composite material similar to a sandwich just with higher stiffness properties. However good compaction is difficult to achieve.
- Near-zero CTE, hence the fabric has good processing compatibility with carbon fibers.

### Processing guidelines

The principle of powerRibs is to create a rib structure on the surface of the composite part. Therefore it only works with an open mould process, i.e. with the mold on one face and a flexible membrane on the other. For this reason, different processes are recommended:

#### Manufacturing with wet lay-up:

Laminate your fabrics in the mold as usual  
Be sure that there is a little excess resin quantity on the fabrics (~200-250g/m<sup>2</sup>)  
Place dry powerRibs on the top of impregnated fabrics  
Place vacuum bag (very flexible, self-releasing) directly on the fabrics, without peelply or flow media.  
Full vacuum: at first the ribs act as air circulation media. Later they get impregnated with excess resin (usage of low viscosity resin is highly recommended).

#### Manufacturing with prepreg:

Place your prepreg fabrics in the mold as usual  
Be sure that there is excess resin quantity in the prepregs (~150-200g/m<sup>2</sup>), otherwise place a resin film on top of it  
Place dry powerRibs on top of the prepreg fabrics  
Place vacuum bag (very flexible, self-releasing) directly on the fabrics, without peelply or flow media.  
Full vacuum: the ribs act first as air circulation media and then get impregnated by excess resin from the prepreg.  
It is also possible to pre-impregnate ribs before placing them on the fabric.  
Check the video "How to make parts with powerRibs prepreg" on our website.

#### Manufacturing with vacuum infusion:

Place your fabrics in the mould as usual  
Place the powerRibs fabric as last layer on the top of other fabrics  
Place vacuum bag (very flexible, self-releasing) directly on the fabrics, without peelply or flow media.  
Infuse the fabrics with the resin.  
Check the video "How to use the powerRibs" on our website.

#### Manufacturing with bladder inflation molding:

Place dry or pre-impregnated ribs over the bladder (elastic bladder)  
Place other fabrics over the ribs. If the ribs are placed dry, the excess resin in the fabric impregnates them.

#### Thermoplastic manufacturing by compression moulding:

PowerRibs preimpregnated with PP as well as preforms with powerRibs and a base material of your choice already bonded together are available. Contact the Bcomp team for further information. To compression mould parts with powerRibs while still conserving the 3D rib effect, a silicon insert is placed on the powerRibs side of the mould. Therefore your tool will need a larger gap size to accommodate the silicon stamp. A 3-4 mm silicon with Shore A hardness between 20 and 30 is recommended. See the video "How to make thermoplastic parts with powerRibs" for more details.